UNIVERSITÀ DEGLI STUDI DI PADOVA

FACOLTÀ DI INGEGNERIA

*Corso di laurea Specialistic*a in
INGEGNERIA AEROSPAZIALE

ANALYSIS AND DESIGN OF A MULTI-PLATE HEAT RADIATOR FOR SPACE AND PLANETARY PROBES

Relatore: Prof. ALESSANDRO FRANCESCONI

Laureando: FRANCESCO COCCO
matricola N. 1063677

A.A. 2014/2015

To my loving parents Luisa and Saverio

Acknowledgements

I would like to thank all the people who contributed to the success of the POLARIS Experiment. I am particularly grateful for the assistance given by Prof A. Francesconi and by Eng F.Branz, L. Olivieri and F. Sansone during the development of the experiment. My gratitude is extended to all the experts from ESA, DLR, SSC and ZARM for their precious advices. A special thanks to the friends of the POLARIS Team Cristian, Federico, Tommaso, Riccardo, Marco, Matteo, Davide and Matteo for the wonderful experience we shared during this passed year.

Abstract

POLARIS Experiment (POLymer-Actuated Radiator with Independent Surfaces) is a technology demonstrator for a new concept of space radiator, which can vary its equivalent thermal resistance through an innovative working principle based on a geometry change. The experiment takes its name from its peculiar dielectric elastomer linear actuation system used to perform the geometry change. This concept of radiator is intended to operate on space and planetary probes which requires a highly flexible and tunable active thermal control subsystem. The experiment aims to evaluate the radiator performance during a stratospheric flight on-board the BEXUS 18 balloon. The stratospheric environment offers a unique opportunity to test this new concept in a realistic context for future applications. This paper presents a detailed description of the experiment analysis and design carried out by a team of university students from the University of Padova. Moreover, the experiment outcomes of the stratospheric flight will be discussed and analyzed.

Contents

List of Figures

List of Tables

Chapter 1

Introduction

POLARIS Experiment (POLymer-Actuated Radiator with Independent Surfaces) is a technology demonstrator, based on a new concept of heat radiator, which can vary its equivalent thermal resistance, exploiting a peculiar dielectric elastomers linear actuation system. POLARIS experiment aims to evaluate the performance of this new concept of heat radiator which allows active thermal control through an innovative working principle based on a geometry change. This concept of radiator is intended to operate on space or planetary probes which have to face variable thermal conditions due to the lack of attitude control, environmental changes or variable internal heat generation. POLARIS Experiment flow on BEXUS 18 balloon (Balloon EXperiment for University Students) in autumn 2014. The balloon, representing a planetary probe without attitude control and exposed to variable environmental conditions, offered the possibility of a realistic test for the radiator performance in an environment similar to the one foreseen for future possible applications on Earth or on other planets with a dense atmosphere such as Venus or Mars.

1.1 Radiator Concept

The design of space probes and satellites has always represented an interesting challenge for the human kind since they need to operate for a long period outside the habitual environment of Earth surface. Spacecraft are exposed to extreme

environmental conditions during their operative live from launch to dismissal, including and harsh vibration, cosmic radiation, high velocity meteoric impacts and hostile thermal environment. The design of thermal control subsystem of a space probe is crucial to maintain the temperatures of its critical components within their operational range. However, because of the extremely variable conditions that satellites face during their operative live, this subsystem must be designed in order to be sufficiently flexible to face all possible external conditions and internal needs of the satellite payload.

In this framework, this paper presents a new concept of heat radiator, which is able to vary its equivalent thermal resistance. Radiators are devices commonly used to dissipate the internal heat generation of a spacecraft toward the external environment. The POLARIS Radiator prototype is composed by three parallel metallic plates, linked together and constrained so that a linear actuation system can separate them or put them in good thermal contact. When the radiator is in its packed configuration, the thermal resistance reaches its minimum and a conductive link through radiator plates enhances the heat exchange. On the other side, in its totally separated configuration, the equivalent thermal resistance is maximized and the radiator behaves almost like a Multi-Layer Insulator (MLI). The last possible configuration foresees a compromise between the previous two in which the second and the third plates of the radiator are stuck together whereas they are separated from the first plate. Figure 3.5 (section 3.1.1, page 19) shows the three possible configurations of POLARIS Radiator. The switch between these conditions allows the change of the system equivalent thermal resistance and therefore it is possible to control the heat dissipated toward the environment.

POLARIS Experiment features a peculiar actuation system which exploits dielectric elastomer actuators. This class of actuators takes advantage of the electric properties of electroactive polymers. ElectroActive Polymers (EAPs) are a particular class of polymers, widely studied in the last decade, which show a deformation in response to an electric stimulation. This particular behavior encouraged new studies to test their potentialities as actuators. Among other EAPs, Dielectric Elastomers (DEs) exhibit the most promising properties. The natural ease of preparing and shaping such DE materials, coupled with their low mass and high energy density, show that they can potentially allow the development of

new actuation technologies. The peculiar actuation system of the experiment is named Dielectric Elastomers Actuation System (hereinafter DEAS). Its characteristic components, the dielectric elastomer actuators, are a recently developed technology that allow an efficient conversion of electric energy into mechanical energy. They are basically built as an electric capacitor, with a thin elastic film of dielectric material between two conductive electrodes (see figure 1.1). When an adequate voltage is applied to the capacitor plates, the electrical force attracts the two electrodes, squeezing the dielectric elastomer which can hence exhibit a deformation.

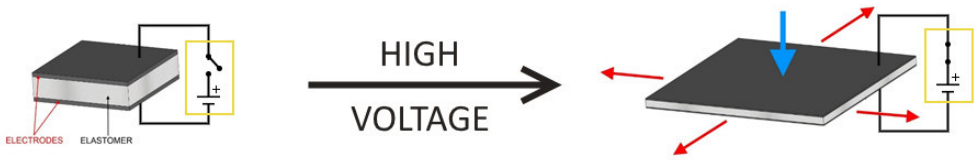

Figure 1.1: Working principle of a DE actuator

For the POLARIS experiment, a particular configuration has been selected for its DE actuators, named rolled DE actuators (figure 1.2). The previously described capacitors are rolled around a compressed coil spring. When the spring is released, it stretches the rolled elastomers until an equilibrium is reached between the opposite elastic forces of the spring and the elastomer. When the actuators are activated, the wrapped film expands, the compressive force of the elastomer relaxes and the actuators show a prevailing deformation along the spring axis until a new equilibrium is reached between the spring and the rolled DE film. A telescopic core has been added to increase the flexural stiffness of the actuators. The telescopic core sustains the spring inside the rolled DE film and offers a cylindrical surface at its extremities where the film can be properly attached. Rolled DE actuators work as an active spring with electrically controllable stiffness. By increasing or reducing the voltage activation level the actuators force exertion can be controlled for a given elongation or vice versa the elongation can be adjusted

for a given external force (Zang, Development of Dielectric Elastomer Actuators and their Implementation in a Novel Force Feedback Interface [2007]). Along its working axis, a rolled DE actuator can exert both contractile and expansive forces. Although the mechanical reliability of this kind of actuator can be enhanced keeping the actuator itself compressed along its axis. This way, the rolled elastomer film is freed by the mechanical stress of the compressed coil spring. Hence the DEAS of POLARIS Experiment foresees a system of springs placed in front of the DE actuators which keep the actuators compressed at any time, both when they are activated or not. This system can extend the operational life of the experiment DEAS and considerably improve its reliability.

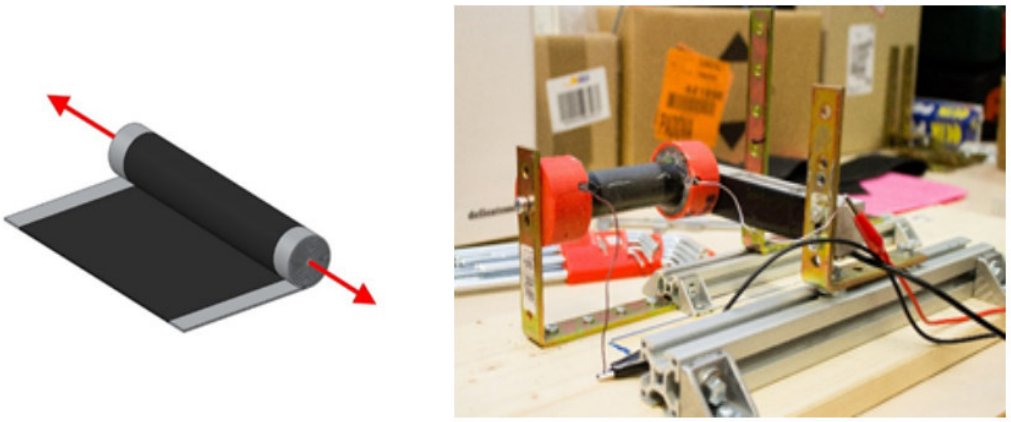

Figure 1.2: Rolled DE actuator. On the left the configuration of a rolled DE actuator is shown, on the right a rolled DE actuator of the POLARIS experiment is mounted on the test bench

1.2 REXUS/BEXUS Programme

The REXUS (Rocket EXperiment for University Students) and BEXUS (Balloon EXperiment for University Students) programmes offer opportunities for university student experiments to be flown on sounding rockets and stratospheric

balloons. Each flight carries a payload consisting solely of student experiments. The REXUS/BEXUS programme is realised under a bilateral agencies agreement between the German Aerospace Center (DLR) and the Swedish National Space Board (SNSB). The Swedish share of the payload has been made available to students from other European countries through a collaboration with the European Space Agency (ESA). EuroLaunch, a cooperation between the Esrange Space Center of SSC (Sweden Space Corporation) and the Mobile Rocket Base (MORABA) of DLR, is responsible for the campaign management and operations of the launch vehicles. Experts from DLR, SSC, ZARM (Center of Applied Space Technology and Microgravity) and ESA provide technical support to the student teams throughout the project (see more on REXUS/BEXUS Website).

The REXUS/BEXUS programme is targeted towards university students in the fields of natural sciences and engineering, who want to fly a rocket or balloon experiment. Participants will experience the full project lifecycle of their experiment, from design and development, to building and testing, to operation and data analysis. At each step of the process, reviews take place to verify the students' work. Moreover, throughout the programme, students have the possibility to have guidance from and work with experts from different agencies.

POLARIS Experiment was selected to participate in the BEXUS 18/19 campaign in December 2013 and was successfully launched on October 10th 2014 from Esrange Space Center near Kiruna, Sweden.

Figure 1.3: POLARIS Experiment and REXUS/BEXUS programme logos

Chapter 2

Experiment Goals and Operative Environment

2.1 Mission Statement

POLARIS is a university student experiment whose purpose is to evaluate the performances of a new concept of heat radiator, which allows active thermal control through an innovative working principle based on a geometry change. Moreover, even if this radiator concept could work with any kind of linear actuation, a system based on dielectric elastomers actuators has been designed and implemented in order to make the experiment scientifically more interesting and challenging. This concept of radiator is intended to operate on space or planetary probes exposed to variable heat fluxes because of their attitude behaviour and operative environment.

2.2 Objectives

POLARIS experiment aims to:

- Study the performances of a new concept of heat radiator which can vary its configuration and equivalent thermal resistance in variable environmental conditions.

- Guarantee, thanks to an active thermal control allowed by the radiator, the thermal steadiness of a dummy payload whose temperature has to remain within a given operational range during a specific phase of the flight.
- Verify the correlation between the numerical model used to predict the thermal behaviour of the dummy payload and the measured data, in order to validate the theoretical model and verify the performances of the radiator prototype.

2.3 BEXUS Environment

The POLARIS experiment has been designed and built in order to ensure its proper functioning during a whole flight on a stratospheric balloon. The experiment can operate for an extended period in a stratospheric environment and during the ascending and descending phases of the flight. A stratospheric flight is characterized by mechanical and thermal loads that can lead to components or system failures if not countered properly. Hence, POLARIS experiment has been designed taking into account all possible mechanical and thermal loads which can occur during a stratospheric flight. Hence, the experiment has been designed and tested taking into account all possible mechanical and thermal loads following described.

2.3.1 Balloon Flight Configuration

Figure 2.1 shows a typical BEXUS flight train and highlights its main components. At the bottom of the flight train, the gondola contains the experiments and provides electrical power and radio link. At the end of the flight, an explosive cutter separates the balloon from the rest of the flight train. A parachute system brings down everything below the cutting device. The EBASS (Esrange BAlloon Service System) provides the primary tracking method of the flight and transmits the balloon location with its own GPS receiver. Both the balloon envelope and the payload are equipped with an air traffic transponder and altitude encoder (Air Traffic Control or ATC). These transponders are switched off by a barometric switch at around 23 km. In addition a Globalstar simplex transmitter is located

on the balloon, and sometimes additionally on the gondola and flight train. These transmitters are used primarily for redundancy and to aid recovery of the balloon material. The radar reflector is also used to locate the balloon after landing. More details about the BEXUS system can be found in the BEXUS User Manual [2014] on REXUS/BEXUS Website).

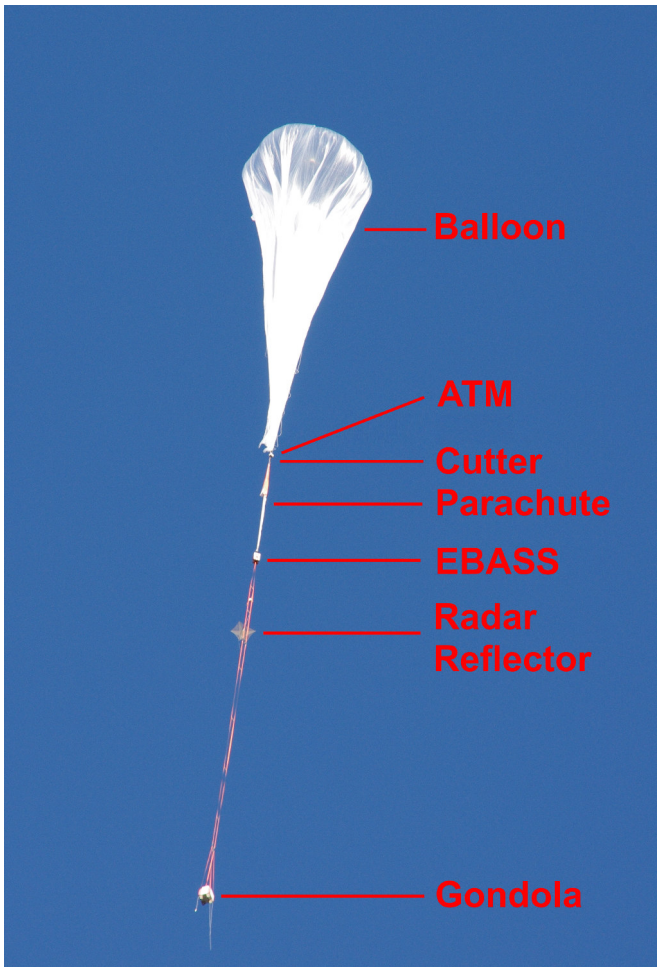

Figure 2.1: BEXUS flight train and its components

2.3.2 BEXUS Flight Profile

Figures 2.2 and 2.3 show the altitude and external air temperature profiles of the BEXUS 18 flight together with those of some previous BEXUS flights. The floating time requested for the POLARIS mission was three hours. However the weather conditions (in particular the strong high-altitude winds) forced a premature cut-off of the balloon and hence a shorter flight duration. The BEXUS 18 floating time was about one hour and ten minutes. The experiment timeline was subjected to some alteration compared with its nominal in order to fulfill the experiment objectives as far as possible despite the shorter mission duration. Section 4.2 contains more details about nominal and real timelines for the balloon flight of POLARIS Experiment.

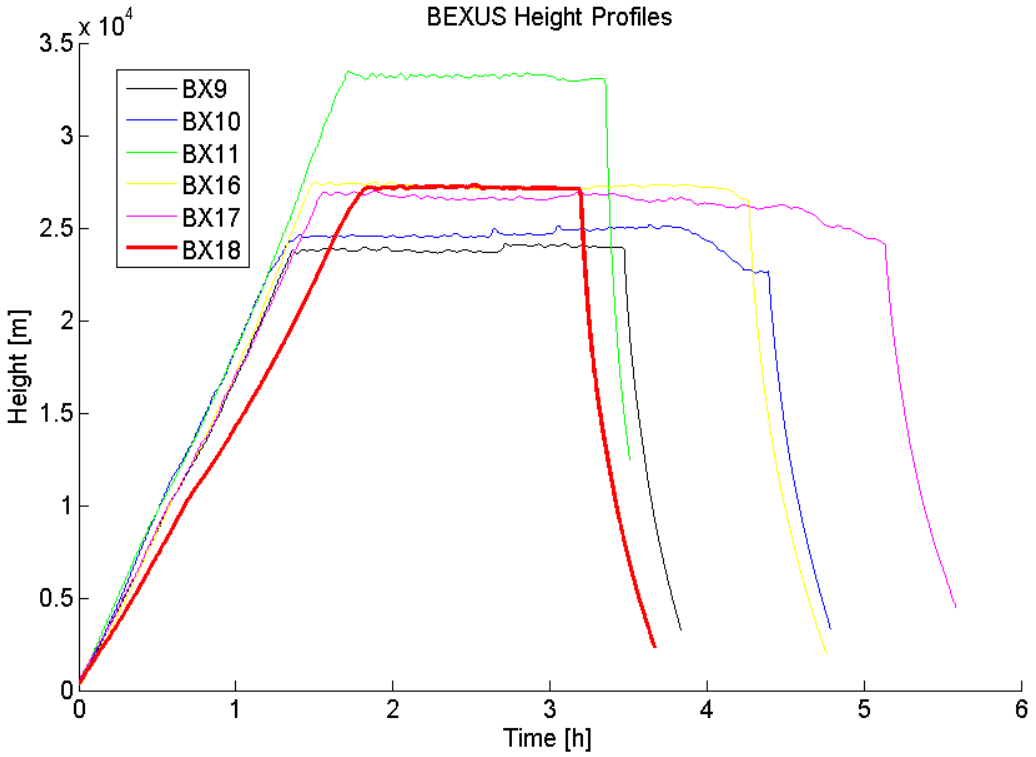

Figure 2.2: Typical BEXUS height profiles during flight

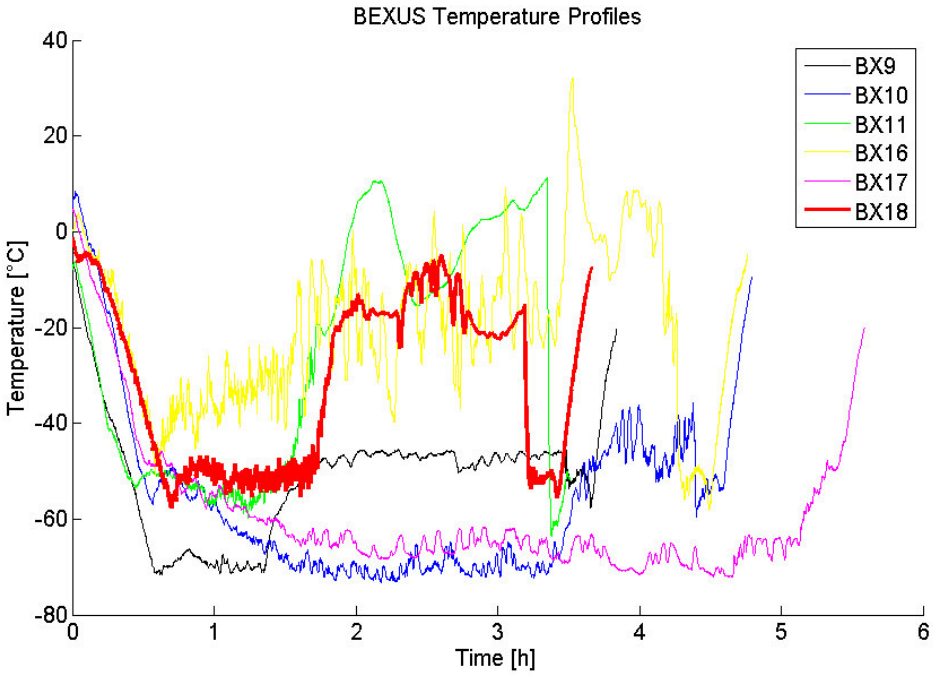

Figure 2.3: Different external air temperature profiles measured during a BEXUS flight

2.3.3 Mechanical Loads

Balloon launch and gondola landing are the most critical phases when the gondola undergoes the heaviest mechanical loads. During its launch, the balloon is released by a launch vehicle and experiments inside the gondola can be subjected to strokes and strong vibrations. An impact with the launch vehicle is also a possibility, although it is really unlikely to happen. The landing velocity is approximately 7 - 8 m/s. This is equivalent to a drop from about 3 m. There is shock-absorbing material at the bottom of the gondola which lowers shock loads at landing. Nominally, the landing is gentle with no damage to the experiments (BEXUS User Manual [2014], section 4.4). Following the BEXUS User Manual [2014] guidelines, the experiment has been designed in order to support nominal acceleration loads of $-10\,g$ vertically and $\pm 5\,g$ horizontally.

2.3.4 Thermal Loads

As can be seen in figure 2.3, external air temperature conditions can vary significantly during different BEXUS flights. Experiments on a BEXUS gondola can be subjected to external temperatures that can drop below -70^oC. The balloon attitude behaviour makes the experiments face variable sun exposure. A temperature gap of more than 70^oC can be measured between different external walls of the experiments, depending on their light exposure. Moreover, the balloon could remain for a long period on the launch pad during the pre-launch and the countdown phases before the flight (BEXUS User Manual [2014], section 6.4). Thus, a proper thermal control system is needed in order to ensure that the internal temperature of the experiments remains within the operative range of all their components for the whole duration of the flight and preflight activities. Section 3.3.1 contains a detailed description of the thermal control subsystem of POLARIS experiment.

Chapter 3

Design

In this section, a detailed description of all the experiment subsystems will be presented And design decisions will be analyzed and justified. POLARIS Experiment is a complex system composed of many different parts. Four main subsystems have been defined: Mechanical, Electronic, Thermal and Software. Each subsystem will be described separately in a dedicated section. Figure 3.1 points out some of the main components of the POLARIS experiment which will be further described in the following sections. Commercial Off-The-Shelf (COTS) components have been used whenever possible in order to hold down experiment costs and to reduce time required for design, production and testing of custom components (COTS components reliability is guaranteed within their declared operative range).

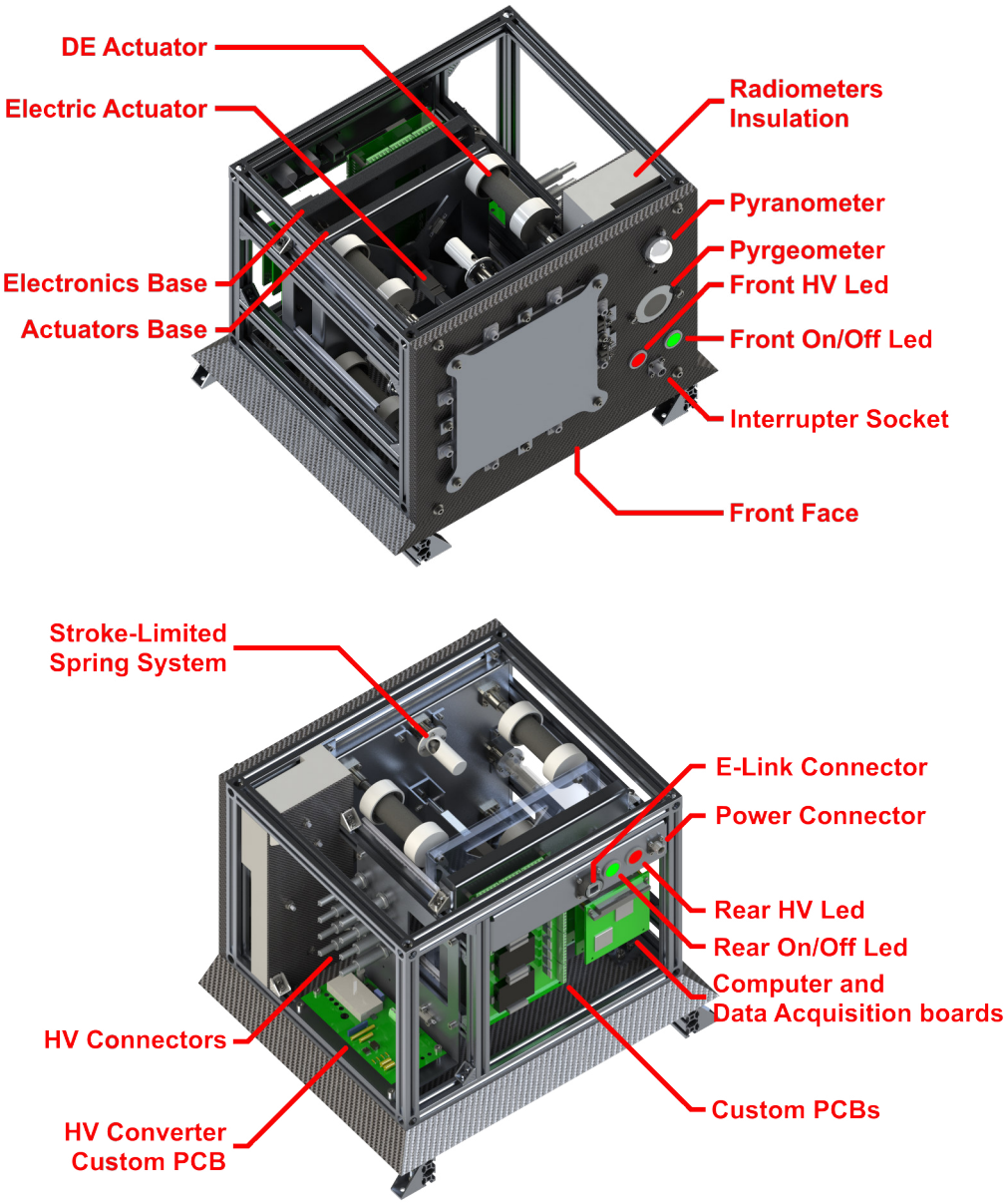

Figure 3.1: POLARIS main components

3.1 Mechanical Design

As shown in figure 3.2, POLARIS Experiment can be ideally split into two main areas. The first, named POLARIS Radiator, represents the payload of the mission while the second, named POLARIS Box, contains the electronics and sensors needed to provide power supply to the experiment and measure its performances. Moreover POLARIS Box protects all internal components from the external environment. The key features which led the mechanical design of the experiment are compactness, ease of manufacturing and assembly, low cost of materials and ease of access to the POLARIS Radiator and to internal components of the POLARIS Box during assembly and maintenance sessions.

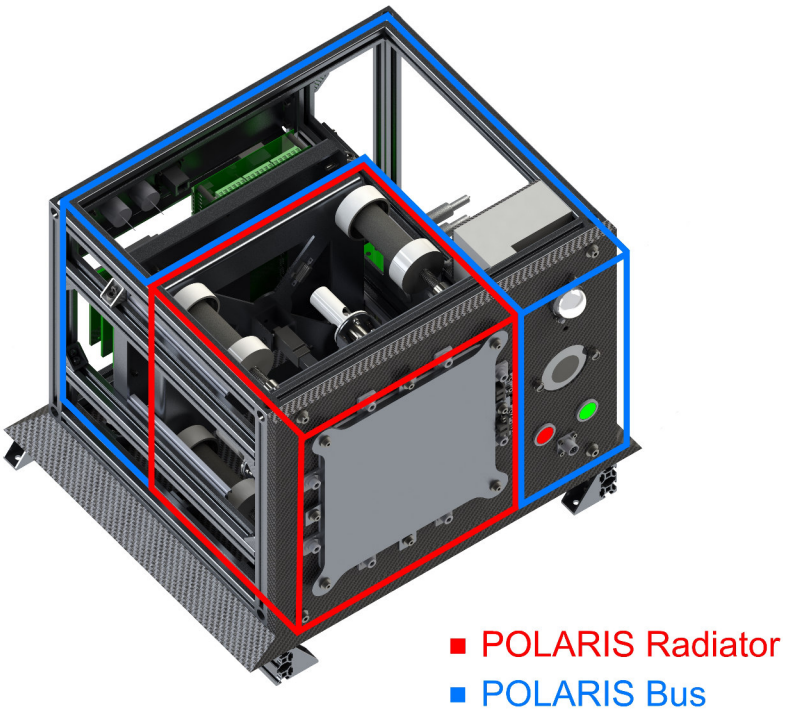

Figure 3.2: POLARIS Radiator and POLARIS Box

3.1.1 POLARIS Radiator

POLARIS Radiator is the core of the experiment and it is composed of three parallel aluminum plates of the radiator itself, their supports and the actuation systems which permit the opening and closure of the plates. Figure 3.3 and figure 3.4 show the POLARIS radiator assembly mounted inside the experiment and on its own.

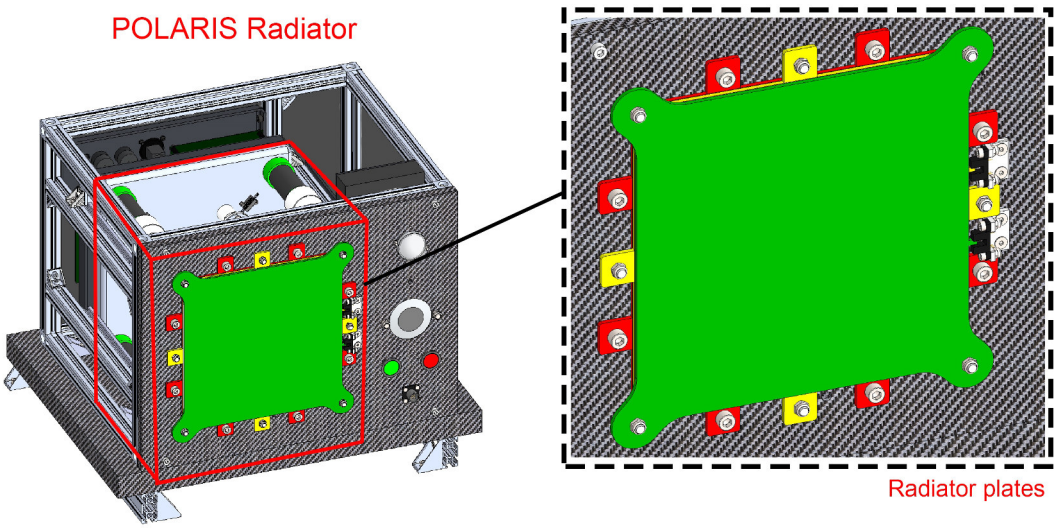

Figure 3.3: POLARIS Radiator detail. Different colors highlight the three independent plates of the radiator.

The radiator plates can shift between three different configurations, as shown in figure 3.5. The switch between these configurations allows the radiator to vary its equivalent thermal resistance and, thus, the heat exchanged with the environment. When the radiator is in its packed configuration (labeled [1] in figure 3.5), the thermal resistance is minimum and a conductive link through the plates enhances the heat exchange. The conductive link is favored by the presence of two thin thermal pads between the three plates fixed onto the external side of the first and second plate. Figure 3.6 shows the thermal pad attached to a spare component of the first plate. On the other side, in its totally separated configura-

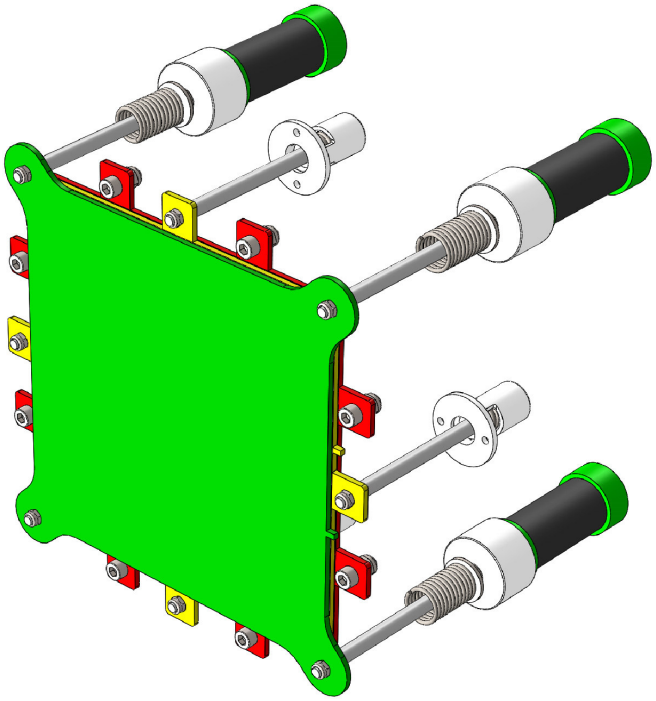

Figure 3.4: POLARIS Radiator assembly and its peculiar actuation system without the supporting frame of POLARIS Box.

tion ([3]) the equivalent thermal resistance reaches its maximum. Heat exchange crosses the gap between the plates by means of radiation or conduction through air of the residual atmosphere. In this configuration, the radiator acts very similarly to a multi-layer insulator and the heat exchange is strongly disadvantaged. The last configuration ([2]) is a compromise between the previous two in which the second and third plates of the radiator are stuck together whereas they are separated from the first one. In its partially separated configuration heat exchange of the radiator is strongly reduced compared with its packed configuration, but not as much as it is in its totally separated configuration.

Figure 3.7 shows a front view of the three plates. The plates share the same basic shape, a $200 \times 200\,mm$ square with smoothed vertices and a thickness of $3\,mm$. The three plates can be distinguished from each other by the different appendages they feature. The first plate has eight $20 \times 20mm$ pierced appendages, two on each side, which allow it to be fixed to the front face of the experiment with as many $M6$ screws. The second plate has four appendages placed in the middle of each side of the plate. Each appendage has a $5\,mm$ square hole in its centre. Finally the third plate has four appendages placed on its vertices, with a square hole in their centres. The plates appendages allow the second and third plates to be connected to their sustaining rods and, hence, to the actuation systems of the experiment as shown in figure 3.4. The shape of the holes permits a secure fastening of the rods and does not require any nut to be mounted in the small gap behind the plates since the rod head is clocked by the plate, unable to rotate, and a screw can be fixed directly in a threaded hole inside the rod. Moreover, the second and the third plates have one more small appendage ($3 \times 3\,mm$) on one of their sides. These appendages allow the experiment to monitor the plates position at any time thanks to a position detecting system as described in section 3.2.1.

Figure 3.8 shows one of the plates rods. The rods transmit the movement from the actuation systems inside the experiment box to the external plates. Rods are made of $PA6+FV30\%$ with a diameter of $8mm$. This material choice guarantees the reliability of the radiator structure. Moreover $PA6$ poliammide and glass fiber (FV) provide good thermal insulation from external environment conditions. Ball bearings support the rods and reduce friction due to their movement, hence

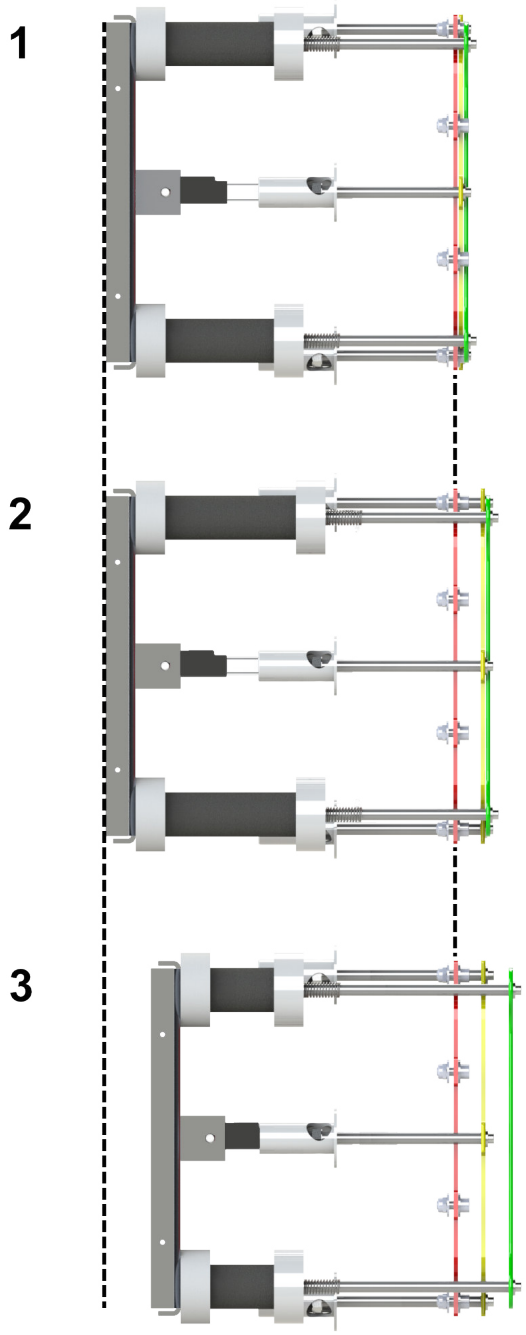

Figure 3.5: Side view of the radiator in its three possible configurations. For sake of clarity, plates distance in separated configurations has been increased in respect to its real value.

Figure 3.6: The internal plate with its light blue thermal pad attached

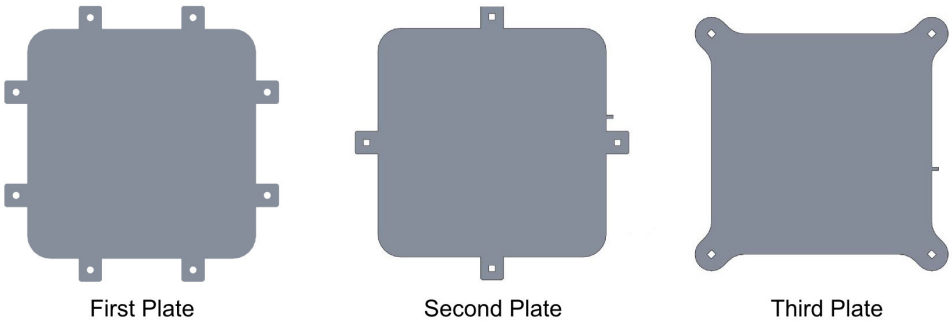

Figure 3.7: Front view of the three radiator plates. Each plate has its peculiar appendages which allow the plate to be mounted in its position on POLARIS Experiment

lowering the force requisite for actuations. The ball bearings are mounted on the back side of an aluminum plate fixed behind the POLARIS Radiator and named Payload Screen Cover (see section 3.1.2 for more details).

Figure 3.8: Radiator rod (on the left) and its supporting ball bearing (on the right). The ball bearings support the rods and reduce friction during their movements.

3.1.1.1 Actuation Systems

Three different configurations are foreseen for the POLARIS Radiator and two actuation systems have been designed in order to allow independent movements of the radiator plates. In particular an independent spring-based actuation system drives the movements of the middle plate whether the actuation is performed by the DE actuators or by the linear electric motor system.

Autonomous Spring Actuation System

The system relies on four Autonomous Spring Actuation (ASA) units. With reference to figure 3.9, the structure of an ASA unit is composed by an ASA support and an ASA plastic box. The aluminum support is fixed to the Payload Screen Cover (see section 3.1.2 for more details) and permits the mounting of ASA plastic box behind one of the ball bearings which sustain the middle plate of the radiator through the ASA rod. The plastic box, mounted on the support, contains a coil spring and represents a fixed base from which the spring can exercise its force. The rod which sustains the middle plate is shaped so that its extremity on the spring side has a smaller diameter than the internal diameter of the spring. The coil spring is placed around this end of the rod and applies its force to the rod. This force presses the middle plate against the external plate while the radiator is in its closed or partially separated configurations. If the external plate moves farther, a bolt screwed along the ASA rod reaches the ASA support and acts as an end-run for the elongation of the coil spring, blocking the mid plate of the radiator. The ASA system passively isolates the movements of the middle plate from those of the external one. This way, the two active actuation systems can switch between the three foreseen configurations of the POLARIS Radiator only by controlling the position of its external plate.

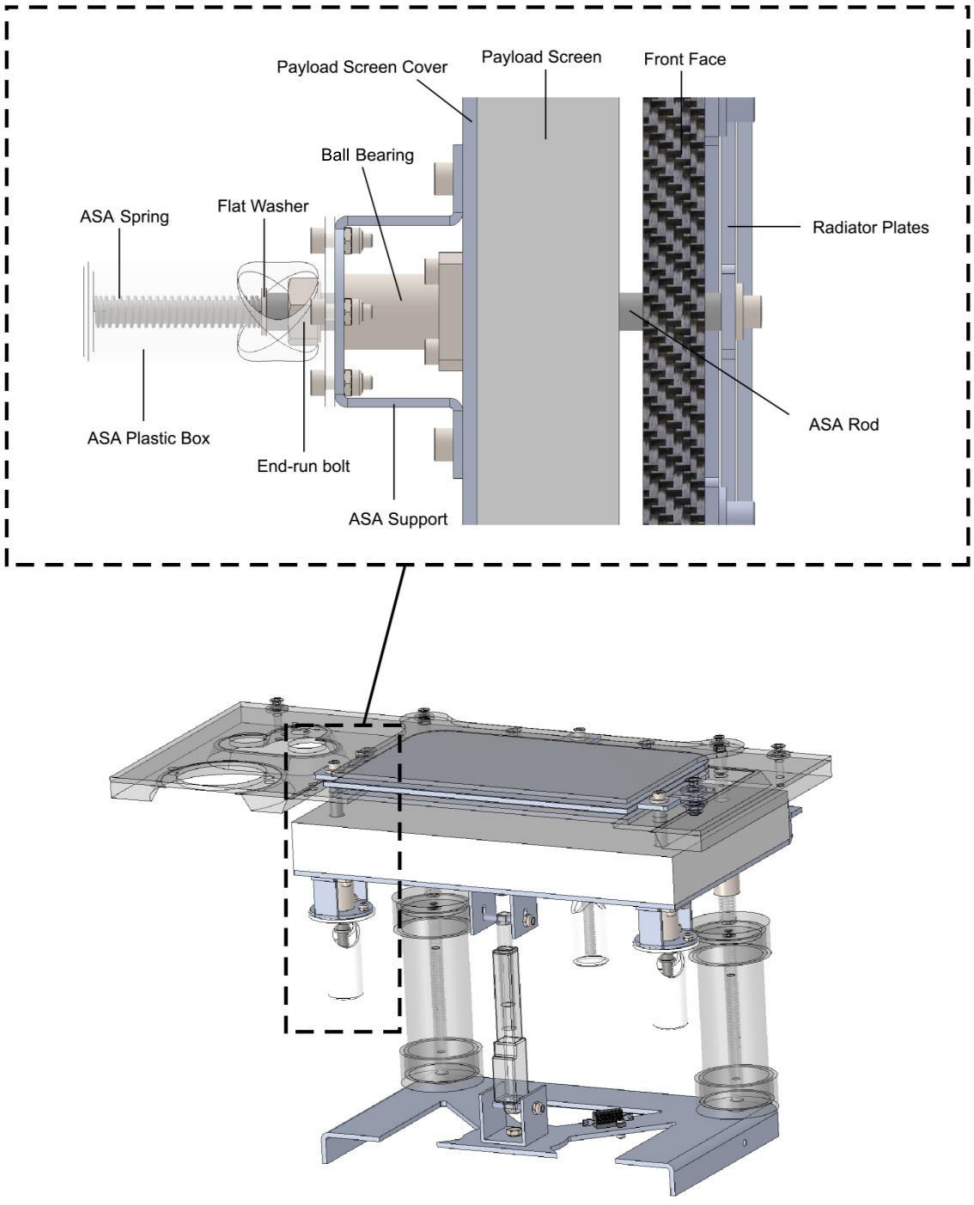

Figure 3.9: Longitudinal section of one of the autonomous spring actuation units and its position behind the POLARIS Radiator. The ASA system drives the movements of the middle plate of the radiator.

Dielectric Elastomer Actuation System

The Dielectric Elastomer Actuation System (DEAS) is the peculiar actuation system of the POLARIS experiment, featuring DE actuators (see section 1.1 for more details). It is composed of four identical units, placed behind the Payload Screen Cover and connected to the vertices of the external plate. Figure 3.10 shows a longitudinal section of a DEA unit. With reference to the figure, the rolled DE actuator is placed between the Actuators Base and the rod connected to the external plate. A screw fastens one of the actuator extremities to the Actuators Base; the other extremity is fixed to the rod. A coil spring is placed between the actuator head and the ball bearing. This spring performs two important tasks. When the DEAS is disabled, it guarantees the closure of the radiator plates, satisfying the pressure requirement between the plates. Moreover, the spring keeps the DE actuator compressed, extending the life and improving the reliability of the actuator itself (see section 1.1 for a more detailed explanation). When the actuator is powered, it pushes against the spring and moves the external plate until a new equilibrium is reached. The force of the ASA springs aids the opening of the external plate until the radiator reaches its partially separated configuration. Unfortunately, the DE actuators are unable to open the radiator plates without the aid of the ASA system springs. For this reason, the DEA system can only be used to switch the radiator between its closed and its partially separated configurations.

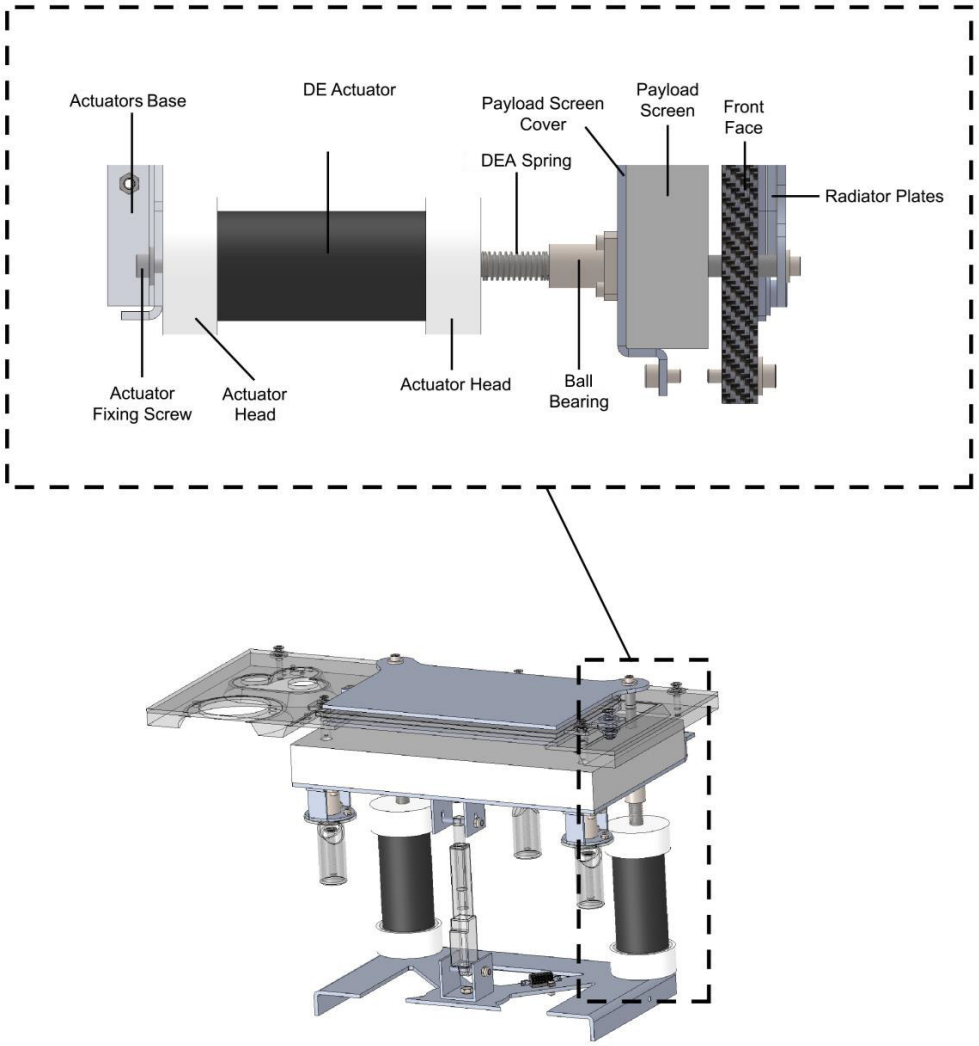

Figure 3.10: Longitudinal section of one of the dielectric elastomer actuation units and its position in the POLARIS Radiator.

Linear Electric Motor Actuation System

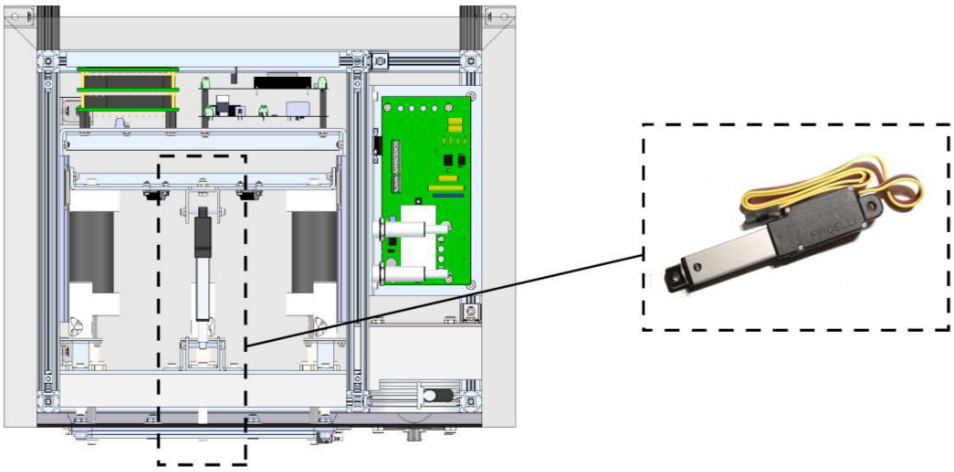

Figure 3.11: Upper view of the linear electric motor actuation system inside the experiment and a detail of its *Firgelli L12-I* electric motor

The Linear Electric Motor (hereafter referred to as LEM) system features a *Firgelli L12-I* linear electric motor placed between the Payload Screen Cover and the Actuators Base. The Actuator Base is fixed on four *IGUS Drylin® N Series 27-LLYZ* carriages. The four carriages can move along as many *IGUS* rails, mounted on the experiment structure. The *IGUS* rail-carriage system leads to several advantages such as lightweight, self-lubrication and dry-running. Hence, the Actuators Base is free to move along the mounting direction of the *IGUS* rails (vertical direction in the upper view of the experiment shown in figure 3.11). This design also guarantees the parallelism of the Actuators Base with the radiator plates, blocking its rotation short of small angles due to component tolerances and inaccuracies during the experiment assembly process. When the LEM is powered-off, it can statically sustain a force of up to 150 N. Hence, the the LEM is capable of holding the Actuators Base in position without any power consumption. When the experiment requires the radiator plates to be moved to the totally separated configuration, the LEM pulls the Actuators Base towards the Payload Screen Cover. The Actuators Base compresses the DEA system

and separates the radiator plates. In figure 3.5 it is possible to see the totally separated configuration (3) of the radiator and the position of the Actuators Base in this configuration. The LEM can also move the plates to the partially separated configuration, working as a backup solution for the DEA system.

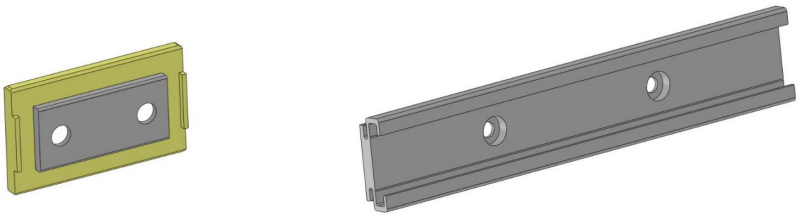

Figure 3.12: A carriage (on the left) and a rail (on the right) of the *IGUS* system. The *IGUS Drylin*® technology allows a lightweight, self-lubricated dry-running of the carriage along the rail.

3.1.2 POLARIS Box

A frame, assembled with *Bosch Rexroth* aluminum profiles, represents the main structure of the POLARIS experiment (see figure 3.13). This aluminum modular profile system offers several advantages such as a lightweight duty structure, modularity and easiness of assembly. In each corner of the frame a corner cube connector (figure 3.14D) is used to constrain three different profiles. The entire main frame is fixed with eight corner cube connectors. Two $260\,mm$ long profiles are constrained in vertical position on the front side and on the back side of the frame, making a $260 \times 260\,mm$ window where POLARIS Radiator can be placed. The two profiles are constrained to the frames with $20 \times 20mm$ Bosch gussets (figure 3.14C). The whole structure can be fixed by means of $M5$ screws.

The Actuation Base is fixed to the experiment box frame as described in section 3.1.1.1 as well as two shelves where the experiment electronics can be mounted. The first shelf is dedicated to the high voltage PCB and to its connectors while the second one sustains all the other PCBs, the on-board computer

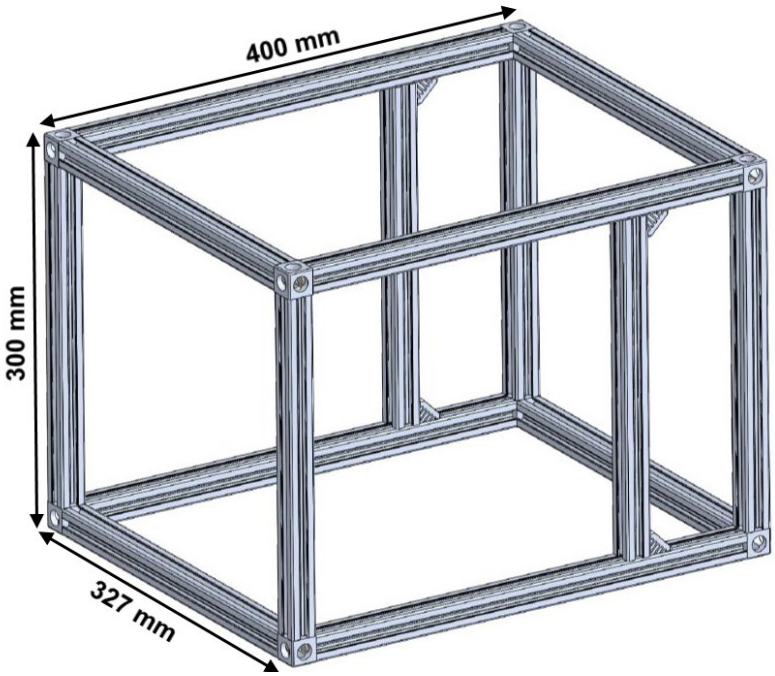

Figure 3.13: Experiment Box frame

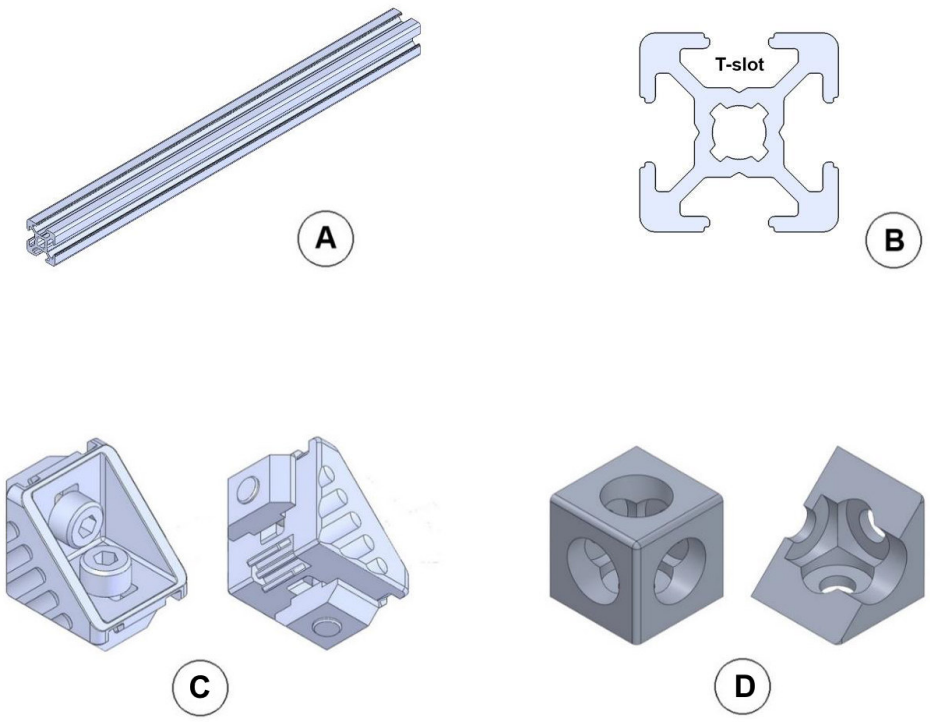

Figure 3.14: *Bosch Rexroth* aluminum modular system. Above, a *Bosch Rexroth* profile (A) and a detail of its section (B). Below two different types of connectors: a $20 \times 20mm$ gusset (C) and a $20 \times 20mm$ corner cube connector.

and the data acquisition boards.

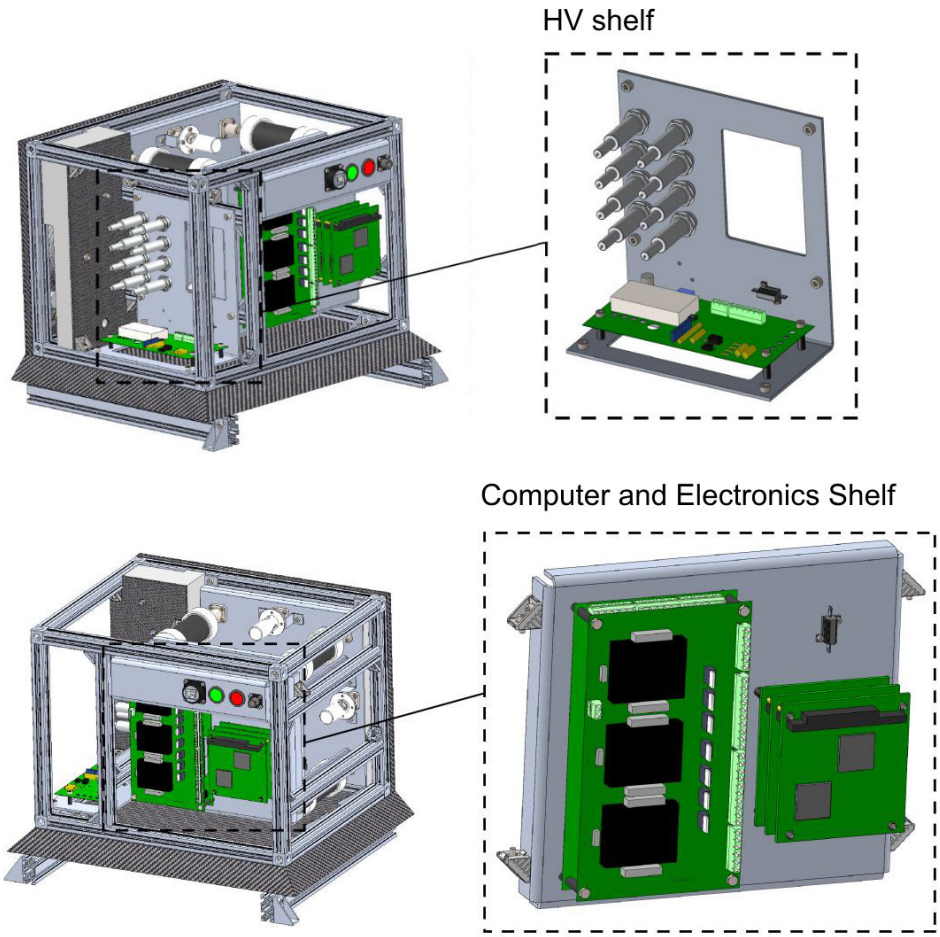

Figure 3.15: Electronics Shelves. Above the shelf dedicated to the high voltage PCB and its connectors, below the shelf for the on-board computers and other electronic components.

An insulating shell is mounted on the external faces of the frame. The shell is composed of a front face panel and five other 30 mm thick composite panels covering all other sides of the experiment box. The main purpose of these panels is to insulate the internal components of the experiment from the external environment. For this reason the panels are composed of a carbon fiber shell with an

expanded foam inside, named Rohacell® 51 IG, which guarantees the thermal insulation of the experiment. Each screen is fixed to the box frame by means of four M5 plastic screws which also prevent heat exchange. When two panels have to be mounted one next to the other, the common edge of both panels has a 45° chamfer which prevents the deterioration of the carbon fiber surface due to screens sliding during assembly or maintenance sessions. On the back side of the experiment is placed the Rear Connections Panel (see figure 3.17). The Rear Connections Panel is placed on the back side of the experiment and it can be reached through a hole in the back side of the insulating shell of the experiment. Two connectors and two LED indicators are placed on the panel. The first connector is an 8-4 insert arrangement *Amphenol* $PT02E8\text{-}4P$ which allows the experiment to be powered by the $28\,V$ external power source of the BEXUS gondola. The second is an *Amphenol* $RJF21B$ Ethernet connector which permits the connection with the $E - Link$ network provided to the experiments during the flight. Finally the two LED indicators show if the experiment and the high voltage circuit are powered on.

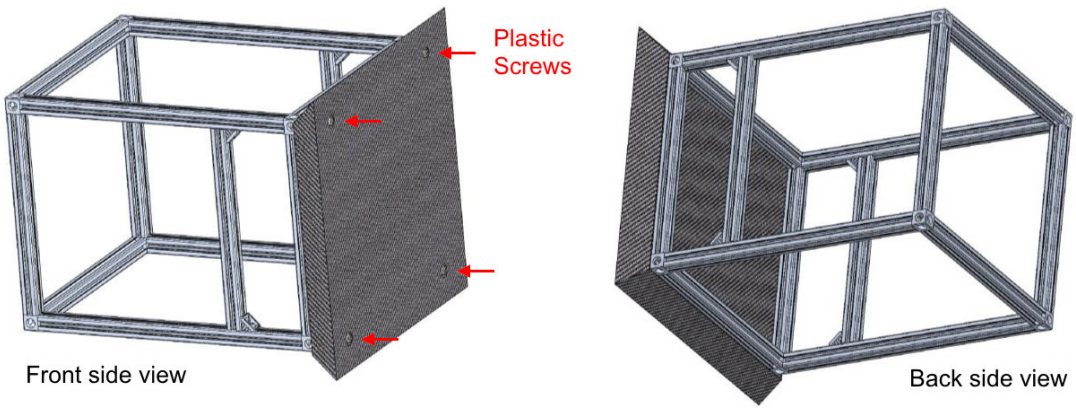

Figure 3.16: Mounting detail of the thermally insulating shell on the box frame

The front face is where the POLARIS radiator is placed and it also holds in position most of the external sensors of the experiment. It has required a more detailed design in order to guarantee both the mechanical stiffness and the thermal insulation required for this element. The front face is a $400\times300\times13\ mm$

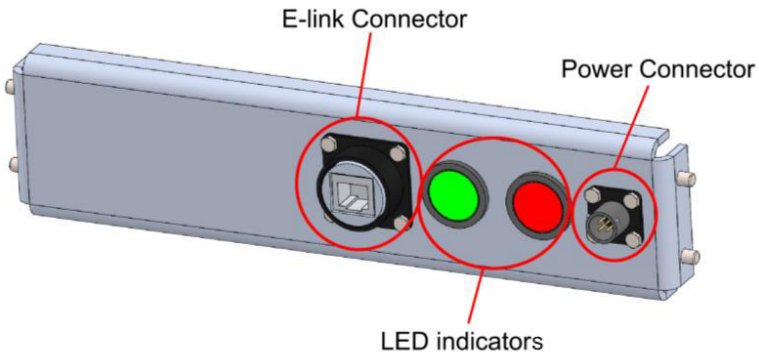

Figure 3.17: Rear Connection Panel of the experiment. The Rear Connection Panel allows the experiment to be powered by the 28 V external power source of the BEXUS gondola and to be connected to the provided $E - Link$ network. Moreover two LED indicators show if the experiment and the high voltage circuit are powered on.

composite panel assembled with a 3 mm thick carbon fiber panel and a shaped 10 mm thick Rohacell® 51 IG panel, both enveloped and held together with an additional thin layer of carbon fiber. The 3 mm of carbon fiber provide the mechanical stiffness while the Rohacell® 51 IG the thermal insulation. Figures 3.18 and 3.19 show two different views of the front face panel, as it can be seen from outside and from inside the experiment. With reference to figure 3.18, on the left, it is possible to see the window for the POLARIS Radiator. Once the experiment is mounted, it is possible to reach the area behind the first plate of the Radiator from this window, enabling easy positioning, assembly and maintenance of the dummy payloads and the temperature sensors. Surrounding the window there are several holes which allow the mounting of the Radiator and provide a passage for cables of the external sensors. In particular, eight $\phi 8\, mm$ holes, one on each corner and one in the middle of each side of the window, are designed for the rods which hold the radiator plates. Eight more $\phi 5.5\, mm$ holes allow the fixing of the first plate by means of as many $M5$ screws and nuts. Finally, four more holes are foreseen for the sensor cables. On the right side the two larger holes are where the radiometer sensors are located. Two $\phi 5.5\, mm$ holes for each instrument allow its fixing by means of two threaded bars. Between the

two radiometers, a $PT100$ RTD is placed to evaluate the external temperature. The three holes in the lower part of the front face are the foreseen location for two more LED indicators for the experiment and for its switch. Finally, on the corners of the front face panel, four holes allow the fixing of the panel directly to the experiment box frame by means of four plastic $M5$ screws.

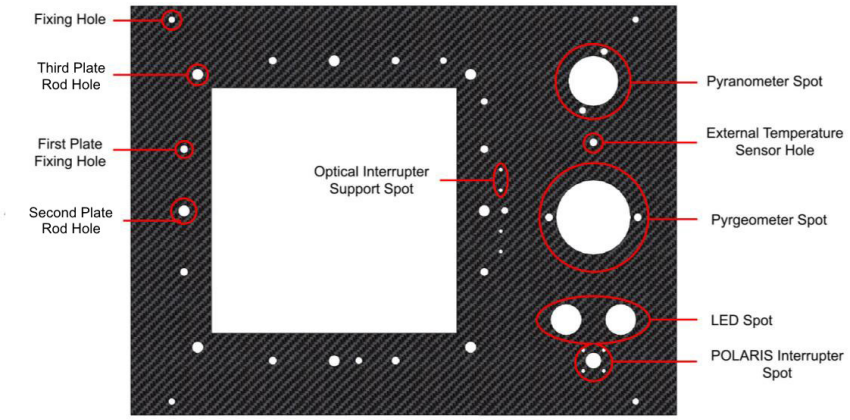

Figure 3.18: Front view of the front face panel

Internal Thermal Insulation

Since both the POLARIS Radiator and the radiometer sensors need to be to be thermally insulated also from the thermal fluxes internally generated from the experiment electronics, two insulating walls have been foreseen to protect these sensitive components. Behind the radiator window a shaped Rohacell® 51 IG foam wall (figure 3.20A) protects the POLARIS Radiator from the internal thermal fluxes. The wall is held in position by the Payload Screen Cover (figure 3.20B) fixed to the experiment box frame. The cover also allows the fixing of the ball bushings used to reduce the actuation friction as described in section 3.1.1.1. Behind the radiometers, another foam shaped wall has been designed (figure 3.21). This wall is also required to sustain the weight of the two sensors and to fix the threaded bars used to hold them in position. For this reason, a carbon fiber panel has been added behind the wall to increase its mechanical stiffness and allow to fasten the nuts on the threaded bars

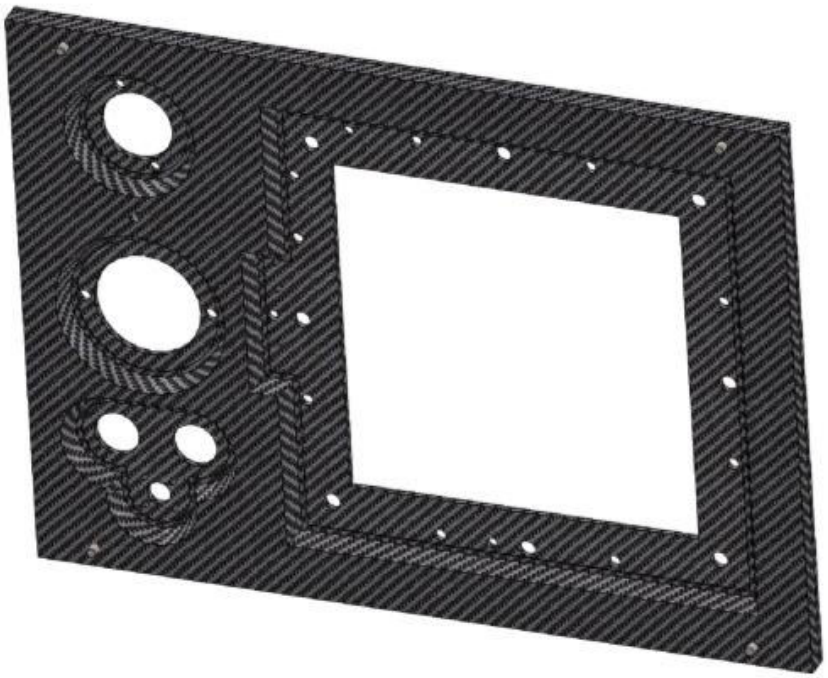

Figure 3.19: Rear view of the front face panel

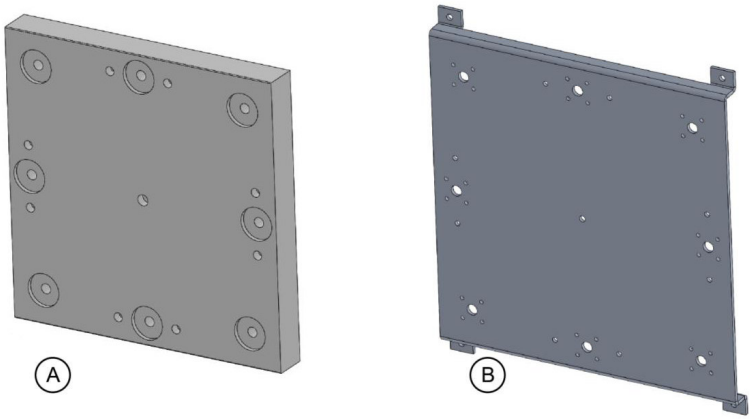

Figure 3.20: The insulating wall of the POLARIS Radiator and its aluminum cover

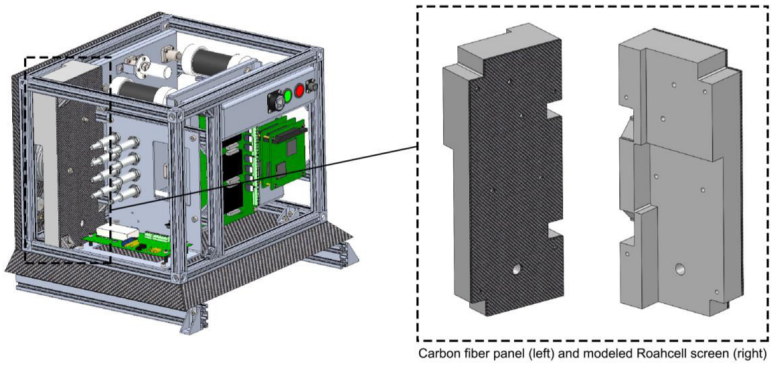

Figure 3.21: The insulating wall of the radiometer sensors

3.2 Electronic Design

The control subsystem of the experiment exploits a PCM-3343 Single Board Computer (SBC), which supervises all operations, receives data from sensors and transmits them to the ground segment. In particular, it controls two data acquisition boards ($Sensoray Model 518$) specifically designed for sensors reading, which handle the whole acquisition process (sensor excitation, signal conditioning, etc.). Based on the collected data, the computer can autonomously turn on and off the dummy payload and change the radiator plates configuration. Nominally, the DEs actuation system performs the switching between the closed and the partially separated configurations of the radiator (see sections 3.1.1 and 3.3.2 for more details about the radiator configurations). The SBC controls the DE actuators position setting their supply voltage. The foreseen supply voltage range can vary from 0 to over $4000\,V$. The high voltage subsystem provides the required voltage thanks to an $EMCO\ C80$ high voltage DC/DC converter which can handle up to $8000\,V$. Otherwise, the electric linear actuator system can perform both the actuation from closed to partially separated and from closed to totally separated configurations and vice versa. Hence, the electric linear actuator can also work as a backup solution in case a failure occurs in the DEs actuation system. Both the HV level and the linear actuator position can be controlled by a voltage signal. The SBC commands two Digital to Analog Converters (DACs) which provide the signal voltages for actuations.

The power stage provides the required voltage levels to all other components of the experiment and it is directly connected to the gondola power source. The $28\,V$ gondola power supply is converted to the desired voltage levels by means of three DC/DC converters. The first converter provides a $12V$ power supply for the linear electric actuator. In case of need, a switch controlled by the SBC can turn off this converter. The second converter provides a $5\,V$ power supply for the SBC and the data acquisition boards. Moreover it provides $\pm 12\,V$ reference voltages needed by the $Sensoray\ 518$ boards. Since this converter supplies the on-board computer, it cannot be switched off. Finally, the third converter provides a $12\,V$ power supply for the HV subsystem. Like the first one, this converter can be turned on or off by the SBC. Some components, such as the dummy payloads,

can be alimented by a $28\,V$ voltage. Hence they are connected directly to the gondola power supply and the SBC can control them by means of several mosfet switches, one for each component.

The high voltage PCB required particular care in order to ensure proper dielectric insulation for the high voltage circuit. The PCB was manufactured with a $2.4\,mm$ thick FR-4 glass-reinforced epoxy laminate and electric traces are spaced for a $20\,kV$ voltage range to prevent arching issues even in low pressure environments. For economic reasons, the same laminate sheet has been used also for the other PCBs, even though if they do not require such insulation precautions.

Three PCBs have been designed and built in order to fulfill the previously described tasks. They have been called Sensor Acquisition Board, Power Supply Board and High Voltage Board respectively, because of the main purpose they accomplish.

3.2.1 Sensor Acquisition

The main purpose of the Sensor Acquisition Board is to gather data from all the different sensors of the experiment and connect them to the two *Sensoray* model 518 data acquisition boards and to the SBC.

One of the two *Sensoray* 518 boards is dedicated to temperature measurements of the radiator plates, employing *class A* $PT100$ RTD (Resistance Temperature Detector) sensors. Sensors are connected in 4-wire configuration to avoid measure errors due to cable resistances. *Class A* RTDs provide $0.33\,K$ accuracy while *Sensoray* 518 guarantees $0.2\,K$ accuracy. Thus the nominal accuracy over temperature measures is about $0.5\,K$. At first, 17 RTD sensors were foreseen for the measurement of the temperature distribution of the radiator plates. *Sensoray* boards feature only 8 channels, each one capable of reading a single 4-wire PT100 RTD, so it is not possible to read all the experiment sensors at the same time. To overcome this limitation a multiplexing-based system was designed. In particular, this system is made of 14 MAX4168 ICs, each one integrating two 4×1 multiplexers. Through this system, each channel of the *Sensoray* 518 can read up to three different RTD at the same time. The SBC can perform the switch between the sensors by means of two digital signals to the selector gates of the

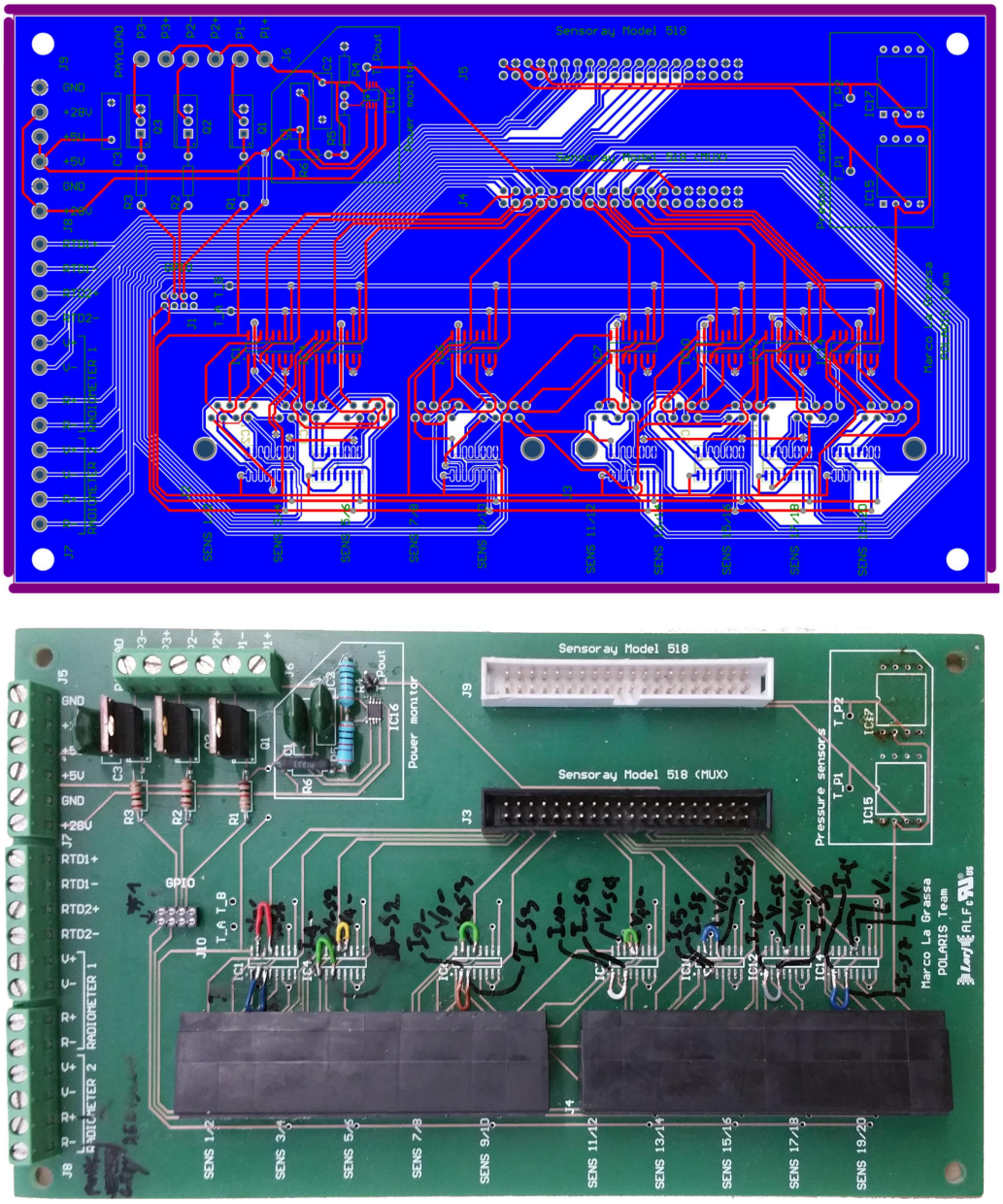

Figure 3.22: Sensor Acquisition PCB Spare component and its schematic

multiplexing system. These signals are generated by two GPIO pins of the computer. However, this solution caused several issues during sensor reading tests. In particular, the acquisition boards provide pulsed sensor excitation RTDs reading. Pulsed excitation minimizes sensor self-heating effects and helps to reduce board power consumption. During tests, the team discovered that multiplexing system entails a parasitic capacity in the reading circuit of the temperature sensors. This parasitic capacity causes a misreading of temperature values, absorbing part of the pulsed excitation current. This problem severely limits the readable sensor number which was lowered from 17 to 8. After these tests, multiplexers have been removed from the Sensor Acquisition PCB and the readable PT100 sensors were therefore connected directly to the data acquisition board.

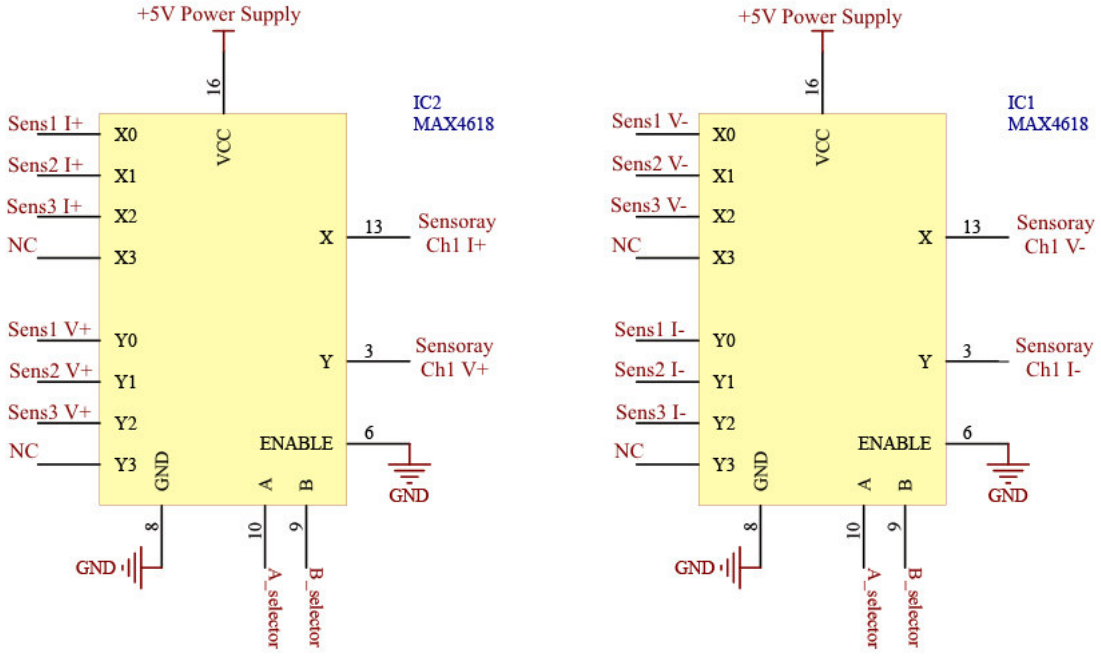

Figure 3.23: Multiplexing schematic for the first channel of the *Sensoray* 518 board. Tanks to the MAX4168 ICs, reading channel can be switch between three different sensors at any time and they can be read with 4-wire configuration.

The second *Sensoray* 518 board handles all other experiment sensors. Among its eight reading channels, two are dedicated to two additional *class A PT*100

RTDs which measure the internal and external temperatures of the experiment. Two more channels are dedicated to air pressure evaluation. Two redundant piezoresistive silicon pressure sensors, mounted directly on the Sensor Acquisition Board, can measure the absolute air pressure from 0 to 160 kPa and guarantee a total error band of 1 % full scale span. Three channels of the *Sensoray* board are needed for the measurement of incoming radiation heat fluxes. Two radiometers, a pyranometer and a pyrgeometer, measure the incoming visible and infrared radiation fluxes respectively. The pyrgeometer requires two separate channels of the acquisition board since both a voltage level measure and a resistance measurement are needed to evaluate the incoming infrared radiation. The resistance measure of the pyrgeometer sensor is required to evaluate its temperature thanks to a NTC sensor placed inside the pyrgeometer. The visible radiation instead can be evaluated with a single voltage level measure from the pyranometer sensor. The last channel of the second *Sensoray* 518 board measures the effective power dissipation of the dummy payloads. A power meter circuit has been designed for this purpose and figure 3.24 shows its schematic.

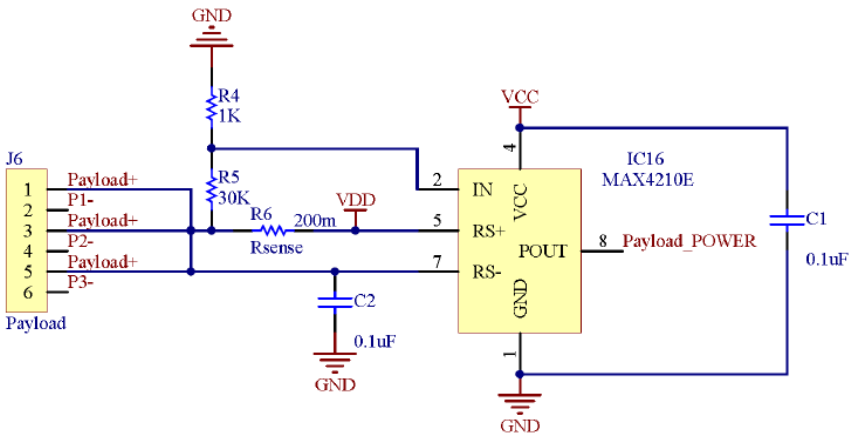

Figure 3.24: Schematic of the circuit which monitors the dummy payloads power consumption

The SBC can directly read two more sensors. Two transmissive optical sensors are mounted on the front face of the experiment and constantly monitor the

plates position, detecting when the appendages of the second and third plates cross their sensing area. Their output is a simple high or low signal and two GPIO pins of the computer can read it. Two zener diodes clamp the output voltage from $+5\,V$ to $+3.3\,V$ which is the maximum input voltage supported by the PCM-3343 GPIO pins. The optical interrupters are placed so that it is possible to determine in which of the three possible configuration the radiator plates are. The first sensor returns a high signal only if the radiator is in its closed configuration. The second one returns a high signal only if the radiator is in its partially separated configuration and a low signal otherwise. Combining these two pieces of information it is possible to determine the radiator configuration. Table 3.1 summarizes the main specifics of the experiment sensors.

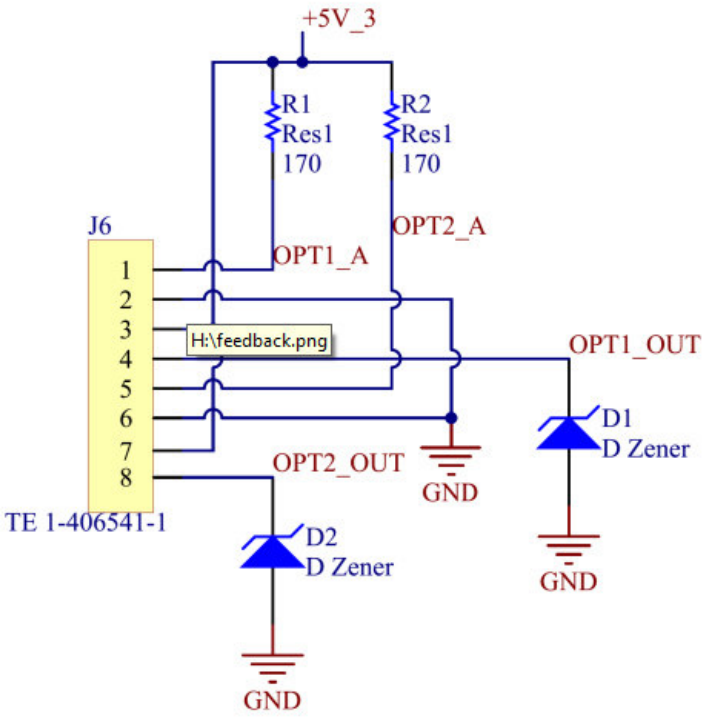

Figure 3.25: Transmissive optical sensors reading schematic

Table 3.1: Experiment sensors

Sensor	**Property**	**Value**
PT100	Type	Temperature Sensor
	Nominal Resistance	100 Ω
	Temperature Range	73 to 873 K
	Temperature Coefficient	3850 ppm/K
	Response Time	1.2 s
	Long-Term Stability	Max drift 0.03% after 1000 h at 873 K
Pressure Sensor	Type	Absolute Pressure Sensor
	Operative Range	0 to 1600 $mbar$
	Accuracy	0.25% full scale span (best fit straight line)
	Total Error Band	Max 1% full scale span
Pyranometer	Type	Net Visible Radiation Sensor
	Operative Range	0 to 2000 W/m^2
	Sensitivity	16 uV/(W/m^2)
	Spectral Range	305 to 2800 nm (50%)
	Response Time	25 s
	Field of View	2π sr
Pyrgeometer	Type	Net Infrared Radiation Sensor
	Operative Range	0 to 1000 W/m^2
	Sensitivity	10 uV/(W/m^2)
	Spectral Range	4000 to 9000 nm (50%)
	Response Time	30 s
	Field of View	2π sr
Power Monitor	Type	Power Meter
	Operative Range	0 to 31 W
	Sensitivity	161 mV/W

3.2.2 Power Supply

The Power Supply Board features three DC/DC step-down converters. These converters are alimented by the $28\,V$ power supply of the BEXUS gondola and provide all voltage levels required by the experiment components. As previously stated, one converter provides the $+5\,V$ and $\pm 12\,V$ voltage levels required by the SBC and by the two *Sensorays* 518 data acquisition boards. The other two converters are dedicated to the linear electric actuator and to the HV converter, both requiring $+12\,V$ for proper operation. The DC/DC converters are mounted on the Power Supply custom PCB and each one has its own EMI filter, designed to achieve $EN55022\ Class\ B$ compliance (see figure 3.27).

3.2.3 High Voltage

The DE actuators need a high DC voltage in order to show sensible deformations. An *EMCO* series $C80$ guarantees a programmable output in the 0-8000 V voltage range. This device can be controlled by the experiment SBC by means of a programming input voltage. As previously mentioned, an Analog to Digital Converter (ADC) provides the required programming voltage level. The SBC controls the ADC with I^2C communication protocol. This protocol allows the on-board computer to control several I^2C devices at the same time, addressing each data packet to its own device. The converter can handle a maximum continuous power of $1\,W$, hence a $100\,M\Omega$ resistor is placed in series with the high voltage output in order to limit the maximum peak current below $125\,\mu A$, ensuring the converter protection. For safety reasons, two red LED indicators light up whenever the HV circuit is powered, one on the front side of the experiment and one on the rear side. The system is designed to automatically switch on the indicators when the voltage level across the DE actuators exceeds a threshold of $\sim 85\,V$. Hence, the switch is independent from the programming input and measures the effective voltage level between the actuators extremities directly. The simplified circuit schematic which controls the indicators is shown in figure 3.29. The voltage across the DEs is scaled down by the HV resistors $R3$ and $R5$ and then sensed by the non-inverting input of an operational amplifier (*ON semiconductors* $LM2904NG$). The latter is configured as a buffer and

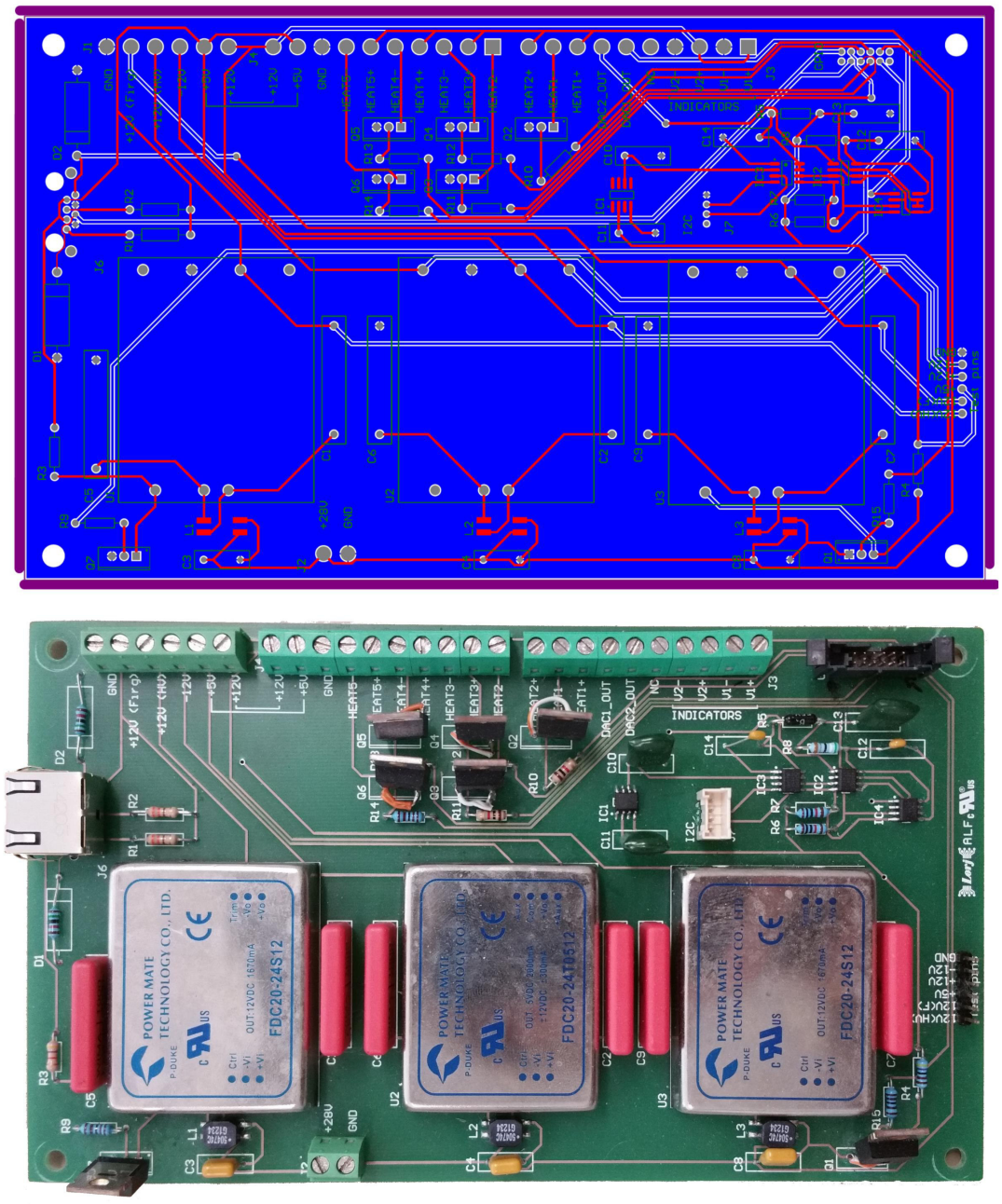

Figure 3.26: Power Supply PCB and its schematic

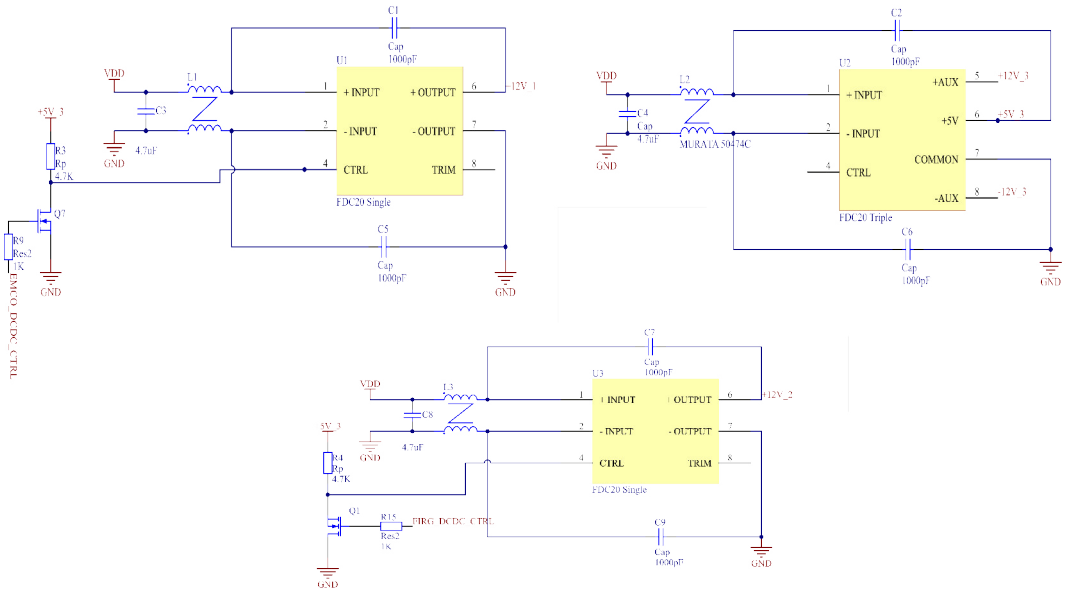

Figure 3.27: Schematic of the filter circuits for the three DC/DC step-down converters of the experiment

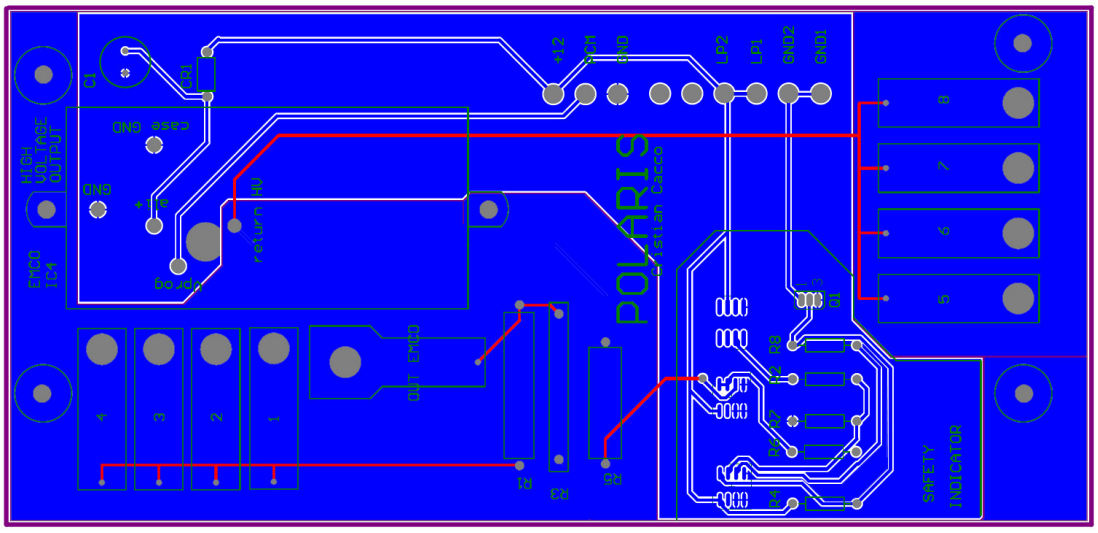

Figure 3.28: High Voltage PCB schematic

it is needed to provide a low-impedance output signal. A comparator (*Texas Instrument LM*293*N*), with an open-collector output, compares this signal to a reference voltage. This reference voltage is provided by a precision voltage reference (*Analog Devices ADR*4533*ARZ*) and two precision resistors (*R*2 and *R*7). When the input signal level exceeds this value, the comparator output returns a high signal, turning on the switch that drives the LED indicators. Finally, feedback resistors *R*6 and *R*8 guarantee a small hysteresis to prevent noise issues.

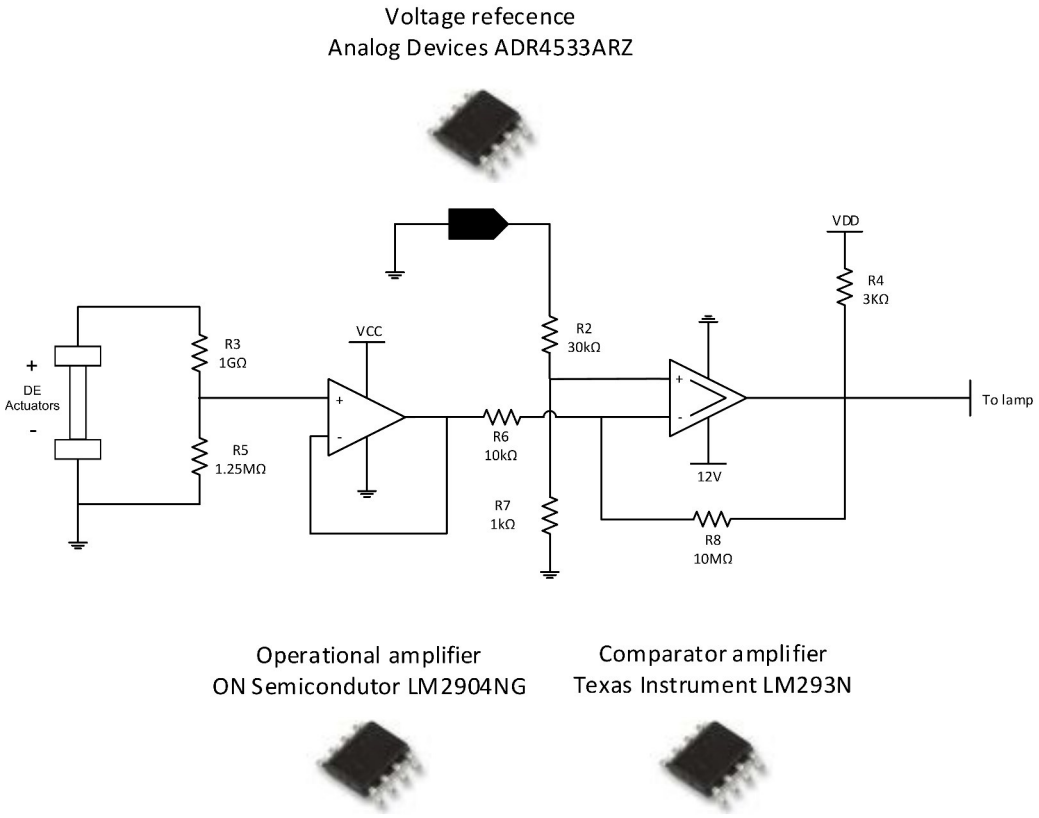

Figure 3.29: LED indicators circuit schematic. the effective voltage level between actuators extremities is measured, switching on indicators, if necessary.

The high voltage power supply needs proper cables and connectors in order to guarantee the dielectric insulation of the whole circuit from the rest of the experiment. The connection between the High Voltage board and the DE actu-

ators features the *LEMO Unipole Y* $3Y$ 410 connectors, which can operate with voltages of up to $10kV_{DC}$ and high voltage cables which can handle up to $12kV_{DC}$.

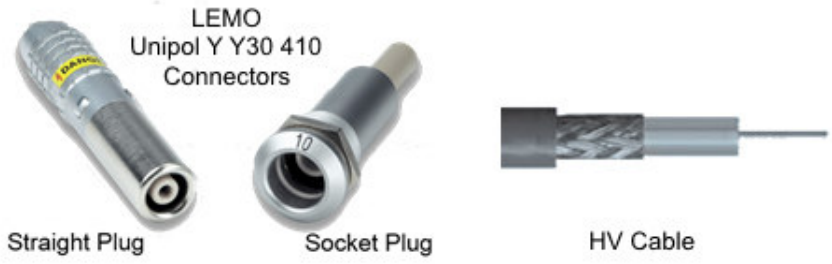

Figure 3.30: High voltage cables and connectors

3.3 Thermal Design

The operational temperature range foreseen for POLARIS Experiment extends from 200 to 310 K. In order to guarantee full system functionality during the whole flight, the experiment has been designed to be able to work properly for a minimum of ten hours within its operational temperature range taking into account the possibility of long holds on the launch pad and extended mission duration (more than the nominal three and a half hours requirement of the experiment). The system is thermally insulated from the external environment, in order to maintain inner temperature higher than outer one during the flight. This allows a more extensive component choice and a wider safety range for operations. The thermal insulation of the experiment is described in detail in section 3.3.1.2. A heating subsystem (described in section 3.3.1.3) has also been designed in order to guarantee wider safety margins.

Table 3.2 shows the operational temperature range of the most sensitive components of POLARIS experiment.

Table 3.2: Operative and storage temperature ranges for experiment components

Component	**Operative Temperature [K]**	**Storage Temperature [K]**
DE Actuators	273-323	273-323
Linear Electric Actuator	263-323	263-333
High Voltage Converter	263-333	253-363
Low Voltage Converters	233-358	218-378
Single Board Computer	233-353	233-358
Compact Flash Memory	233-353	233-353
Data Acquisition Boards	248-358	248-358
Pressure Sensors	233-358	233-358
Radiometers	223-353	203-353
RTD sensors	100-533	100-533
Optical Interrupters	223-353	223-353
Ball Bushings	253-363	223-363
IGUS Linear Guides	233-363	233-363
Dummy Payload Resistors	218-428	218-428

3.3.1 Thermal Control Subsystem

3.3.1.1 Experiment Thermal Behaviour

A numerical simulation has been carried out in order to evaluate the thermal reliability of the POLARIS experiment exposed to the environmental conditions of a BEXUS flight. The experiment has been divided in thirteen different nodes which represent all different parts of the experiment:

- External Insulator Surface
- Internal Insulator Surface
- Box Structure (Bosch Rexroth web)
- Aluminum Payload Screen Plate
- Electronics Plate
- Actuators Plate
- Aluminum Radiators Plate
- Sensors PCB
- Low Voltage DC/DC Converters PCB
- High Voltage DC/DC Converter PCB
- Computer and DAQ Devices
- DEs Actuators
- Linear Electric Motor

Each node is characterized by its own thermal properties (such as conductivity, thermal capacity, etc., which remain constant during the simulation) and its own temperature (which is time-dependent). Conduction, convection and radiation are modelled and cause the heat exchange between different nodes of the simulation and with the external environment. Temperatures of each node are evaluated iteratively using equation 3.1 (Gilmore [1994])

$$T = T_{old} + \frac{q\,\Delta t}{C} \tag{3.1}$$

where T is the new temperature value of the node after the time step Δt, T_{old} is the previous temperature value of the node, q is the heat rating received by the node during the time step and C is the thermal capacity associated with the node. In order to improve the model stability time steps are chosen at each iteration of the simulation so that the maximum temperature variation that any node can experience during a single time step is lower than $0.1\,K$ and in any case up to a maximum of one second. External thermal loads are time-dependent and simulate the environmental conditions on the launch pad and during a BEXUS flight.

Because of the uncertainty or unpredictability of some of the model parameters, two extreme cases have been tested: Worst Cold Case (WCC) and Worst Hot Case (WHC). In both cases, the specific heat capacities of all the components of POLARIS Experiment have been underestimated in order to emphasize the temperature variations. Since the external environment is always significantly colder than the desired internal temperature, the most favourable parameters have been chosen for the WCC whenever an uncertainty arose. On the contrary, the most unfavourable have been chosen for the WHC.

Worst cold case

The changes in temperature of the simulation nodes in WCC can be seen in figure 3.31. Since electronic devices and moving parts are typically the components most sensitive to temperature variations, four horizontal dotted lines highlight their maximum and minimum expected temperatures. The Sensors Acquisition PCB is the electronic component that reaches the lowest temperature, $256\,K$. Comparing this and other evaluated values with those shown in table 3.2 it is possible to see that all electronic components should remain within their operational values for the whole simulation. The DE actuators are the coldest mechanic components. Their temperature remains over $273\,K$ until the sixth hour of flight and never goes under $267\,K$ during the whole simulation. From table 3.2, it is possible

to see that the operational temperature range for these components starts from $273\,K$. However, simulation results have been considered sufficient to validate the DE actuators reliability since:

- The request flight duration for the POLARIS mission is only three and a half hours
- No BEXUS balloon has ever flown for more than six hours
- WCC conditions overestimate the real thermal loads from the external environment
- The WCC simulates a total failure of the experiment heating subsystem of the experiment, which is an extremely unlikely occurrence
- Even in case of failure, the DE actuators do not represent a danger for any person or any other object on-board the BEXUS gondola

Simulation results showed that a heating subsystem with an average required power of about $6\,W$ should be able to guarantee that all experiment components remain within their operative temperature even in the WCC conditions for the whole duration of the simulation.

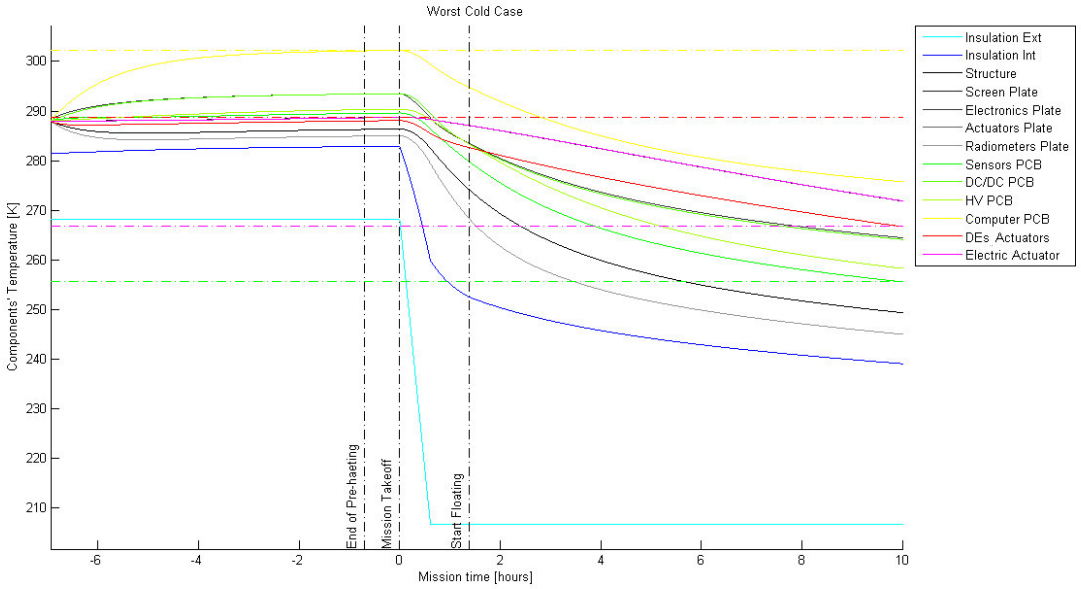

Figure 3.31: Worst Cold Case experiment thermal behaviour

Worst hot case

In this case, a failure preventing the switch off of the heating subsystem has been simulated. Moreover the efficiency of all the electrical components has been severely underestimated and, hence, their heat dissipation increases. Figure 3.32 shows the evolution of the temperatures of the simulation nodes in the WHC. As in the previous case, four horizontal dotted lines highlight maximum and minimum expected temperatures for the most sensitive components. In this case, the computer and the DC/DC converters board are the electronic components that reach the highest temperature, which is lower than $340\,K$. The hottest mechanical component is the linear electric actuator, which reaches almost $300\,K$. In this case, all components remain within their operational ranges for the entire duration of the simulation.

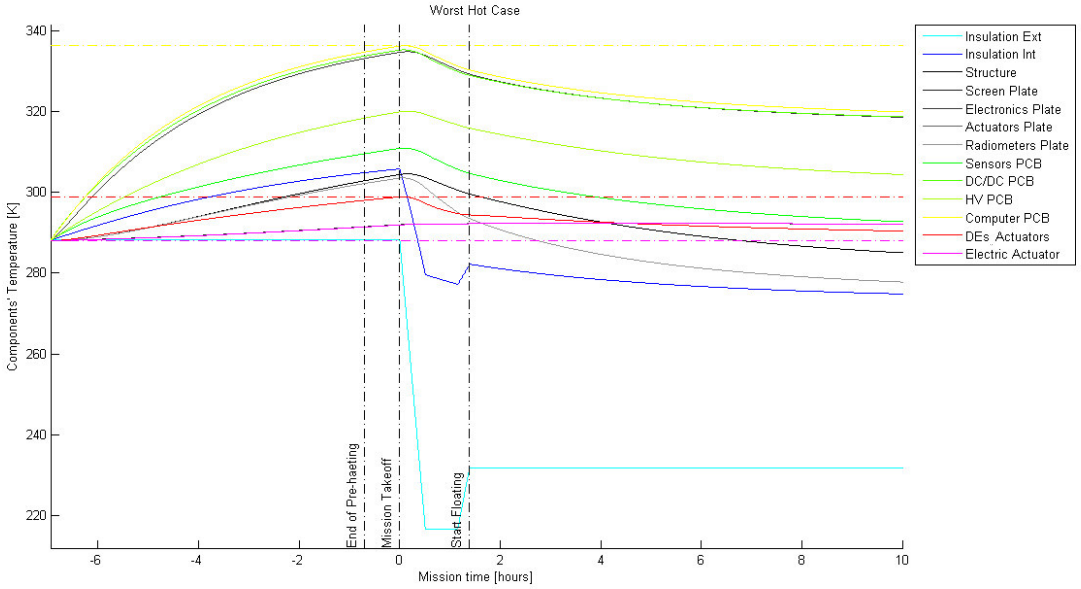

Figure 3.32: Worst Hot Case experiment thermal behaviour

3.3.1.2 Passive Thermal Control

The external shell of the POLARIS experiment has been chosen as the result of a tradeoff between its mechanical stiffness and thermal properties. In particular the front face of the experiment has required meticulous attention since it is the face where the POLARIS radiator is placed and where most of the experiment sensors are held in position. For this reason the front face will be described separately. Five 30 mm thick composite panels cover all other sides of the experiment box. These panels are composed of a carbon fiber shell with an expanded foam inside, named Rohacell® 51 IG. This foam has a thermal conductivity coefficient of 0.033 $Wm^{-1}K^{-1}$ and guarantees the thermal insulation of the experiment and it improves panels bending stiffness. Each screen is fixed to the box frame by means of four $M5$ plastic screws which also prevent heat exchange. Figure 3.16 (see page 31) shows one panel mounted on the experiment structure.

Front face

On the front face of the experiment box there is a 400×300×13 mm composite panel. This panel is the assembly of a 3mm thick carbon fiber panel and a shaped 10 mm thick Rohacell® panel, enveloped by another thin layer layer of carbon fiber which holds them together. The Rohacell® panel protects the aluminum profiles of the front side of the box frame from low temperatures and represents the first thermal shield between the front side of the experiment and the external environment. The carbon fiber panel allows most of the experiment's external sensors to be mounted reliably as described in section 3.1.2. Figure 3.18 and 3.19 (see page 34) show the front face assembly.

3.3.1.3 Active Thermal Control

A heating subsystem has been designed in order to warm up the experiment whenever the internal measured temperature falls below a chosen threshold. Heaters are placed on the experiment aluminum parts in order to quickly increase temperature over a wide surface within the experiment. Simulation results gave a minimum power requirement of about 6 W for the heating subsystem. Since the foreseen power budget allows the heating subsystem to be slightly oversized, it

has been designed to manage up to 10 W during the whole flight in order to be able to work properly even in case of unexpected circumstances. Four power resistors are placed in the experiment as shown in figure 3.33. The heaters can be switched on and off by means of four mosfet switches directly controlled by the on-board software. The latter is designed to manage the heating subsystem autonomously. If necessary, it is also possible to override the automatic behaviour with a ground command.

The heaters subsystem has been designed to be supplied directly from the 28 V power line of the BEXUS batteries, without any voltage conversion. The four mosfet switches allow the enabling of different parts of the heaters circuit independently. An additional switch has been added without any load in order to permit quick modification to the heaters subsystem during the manufacturing and testing phases of the project, if necessary. Figure 3.34 shows the simplified schematics of the heaters circuit.

Several tests, both at system and subsystem level, have been carried out to ensure that this design can guarantee full system functionality of the experiment during a BEXUS flight.

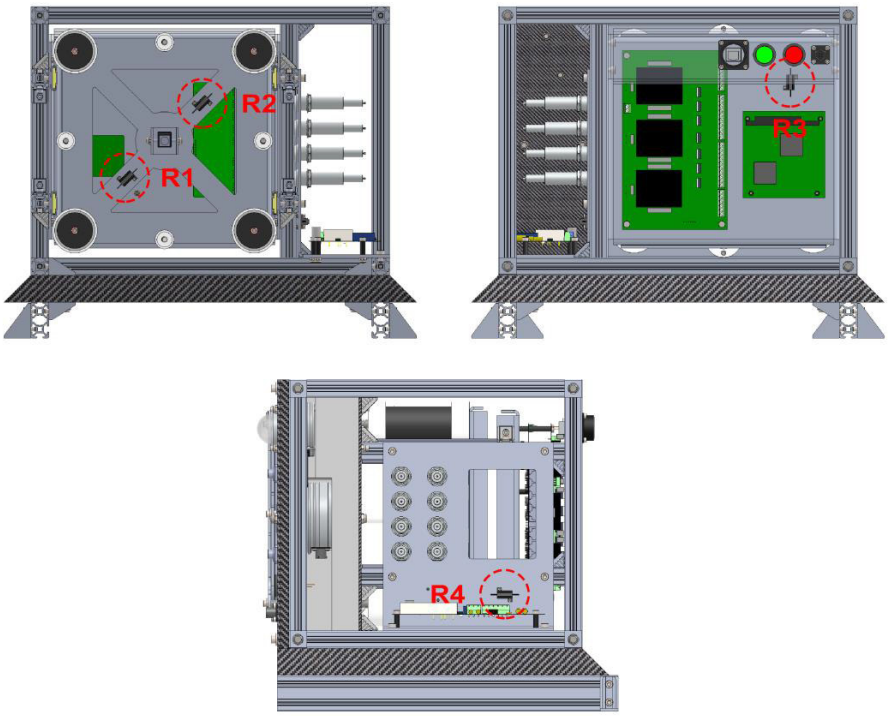

Figure 3.33: Position of the power resistors of the heating subsystem within the experiment

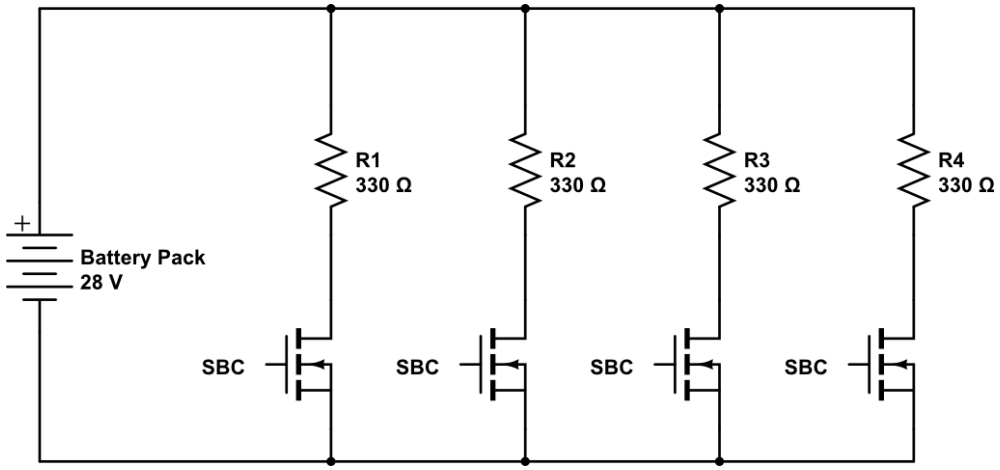

Figure 3.34: Heaters circuit schematic. If necessary, an additional heater can be added with its own switch.

3.3.2 Radiator Design

As previously stated in section 3.1.1, POLARIS Radiator is a device which permits heat dissipation towards the external environment with an adjustable equivalent thermal resistance. The radiator is composed of three parallel metallic plates, linked together and constrained so that an actuation system can separate them or put them in good thermal contact. The switch between these configurations allows the radiator to vary its equivalent thermal resistance. When plates are tightened together, the radiator ideally works as a single plated radiator and conduction promotes heat flux through the plates. On the contrary, if the plates are separated from each other, the radiator behaves like a Multi-Layer Insulator (MLI) and the heat flow is severely reduced. The radiator can also be set in a midway configuration, with the second and third plates tightened together but separated from the first one. In this configuration heat flow is disadvantaged with respect to the closed configuration but not as much as in the totally opened one. Figure 3.5 (see page 19) shows a longitudinal section of the radiator in its three configurations. Plates are represented with different colors to highlight their position. The switch between these three configuration can be achieved by means of one of the actuation systems described in section 3.1.1.

Two thermal pads are placed between the plates in order to increase the heat flux through the radiator when it is in its closed configuration. Figure 3.35 summarizes the main thermal and mechanical properties of the pads. It is possible to see in the graph on the right the dependence between the thermal impedance of the pads and the pressure between the plates. This dependence leads to the closing pressure requirement mentioned in section 3.1.1.1. On the external face of the third plate of the radiator, a black coating has been applied. $3M$ Velvet® Black coating has been selected for this purpose since it guarantees a known and constant emissivity coefficient of 0.97 in visible and infrared spectrum and hence the radiation emitted by the POLARIS radiator can be easily modelled, knowing its temperature. The coating emissivity coefficient is precisely known since it is commonly used in the manufacturing of pyranometer and pyrgeometer sensors. In order to simulate the heat a real payload generates, a heat source is connected behind the first plate of the radiator as a dummy payload. Although

the nominal power of the dummy payload can be evaluated from data sheets of its components, a power monitor constantly measures voltage and current through the resistances and verifies the actual heat ratio generated by the dummy payload. The dummy payload is composed by three $100\,\Omega$ power resistors placed near the center of the first plate with circular symmetry. Each resistor is fed by the $28\,V$ power supply of the BEXUS gondola and nominally generates a heat ratio of $7.84\,W$. Moreover, three dedicated switches can turn each resistor on and off separately. With this design, two power resistors can generate the nominal heat ratio foreseen for the experiment ($15\,W$). The third power resistor has been added as a redundant element to enhance the reliability of the system. This configuration has been preferred to a single power resistor in the middle of the plate for several reasons. Firstly, as formerly stated, the redundancy of the three power resistors increases system's reliability. Moreover, this configuration allows a limited modulation of heat generation since it is possible to switch the three resistors on and off separately. Finally this configuration leaves a free spot in the center of the plate for a temperature sensor to be mounted in this position. At equal positions between the centre and one of the corner, four $PT100$ RTDs are placed along one of the diagonals on the internal side of the first plate. With the same criteria, four more RTDs are attached on the external face of the last plate. These sensors constantly measure the mean temperature of the plates and its spatial distribution over the plates surfaces. Figure 3.36 shows dummy payloads and RTDs positions over the internal face of the first plate and over the external face of the third one.

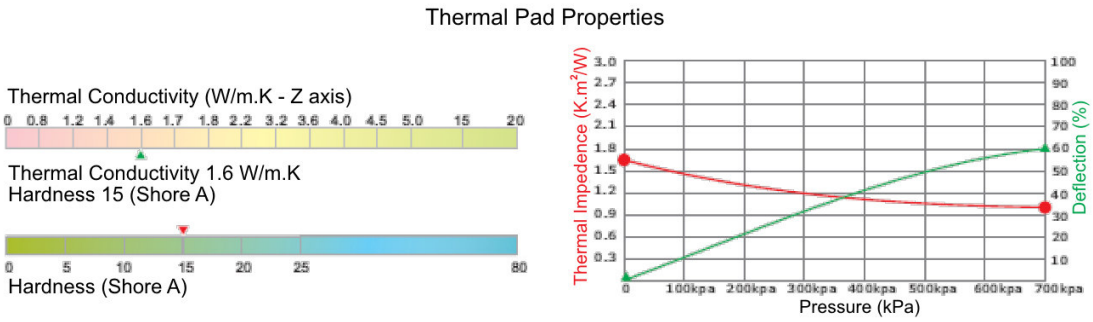

Figure 3.35: Mechanical and thermal properties of thermal pads

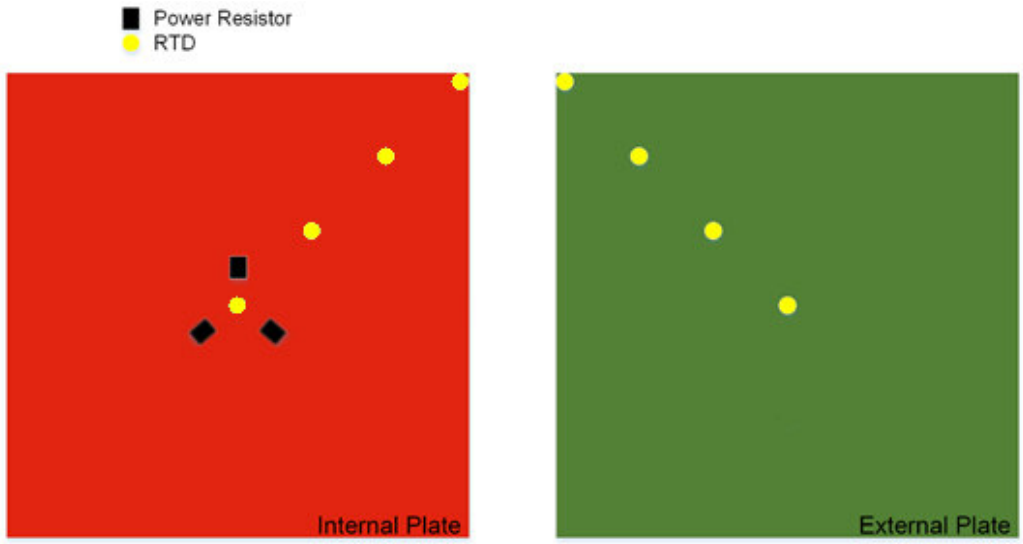

Figure 3.36: Positions of dummy payloads and RTDs over the radiator plates

Radiator behaviour

The core element of the experiment, the POLARIS Radiator, has required detailed analysis and design on its own. Another numerical simulation has been developed to predict the radiator thermal behaviour during a BEXUS flight. The simulation, based on divided differences method, uses the same model of the simulation formerly described (see section 3.3.1.1) to foresee external environmental conditions. The radiator plates have been divided into small elements to be used as nodes for the divided differences method as visually represented in figure 3.37. Thermal fluxes towards each element are calculated at every time step from the initial temperatures of the nodes at current iteration. Hence, temperatures of each node are updated and the simulation proceeds to the next time step. From this model, a parametric analysis has been performed in order to highlight the influence of each parameter over the radiator performance. The program repeatedly simulated the behaviour of the radiator during an entire BEXUS flight switching a single parameter value at each run. The results of this analysis allowed the team to select the best radiator configuration for the experiment. Among others, some of the most relevant parameters for the radiator design are:

- **Number of plates.** As for a MLI, an increase in the number of screens causes a decrease of the heat flux through the radiator in its open configuration. Eventually, this value tends to an asymptote and the decrease ceases. Three plates have been chosen as a compromise between performance and increasing system's complexity.

- **Plates surface.** The radiator dimensions influence heat exchange with the external environment. The power budget for the dummy payloads and the time requirements of the mission set an upper limit for this value. Lower values entail more intense boundary interferences and plate thickness can be no longer neglected. $200 \times 200\ mm$ square plates have been chosen.

- **Plate thickness.** Plate thickness increases the radiator weight without any relevant improvement in radiator performance. Since there is no strict limit for weight, a $3\ mm$ thickness has been chosen in order to guarantee the flatness of the plates.

- **Distance between plates.** In its separated configuration, radiator behaviour is influenced by the distance between the plates since air conduction due to residual atmosphere could not be neglected. A minimum of 3 mm has been set as a requirement for this value.

- **Dummy payloads power budget.** This value directly influences the maximum possible dimensions of the radiator plates. An additional battery pack has been requested from the BEXUS system in order to increase the available power budget. Nominally the foreseen heat dissipation of the dummy payload is 15 W during the floating phase of the flight.

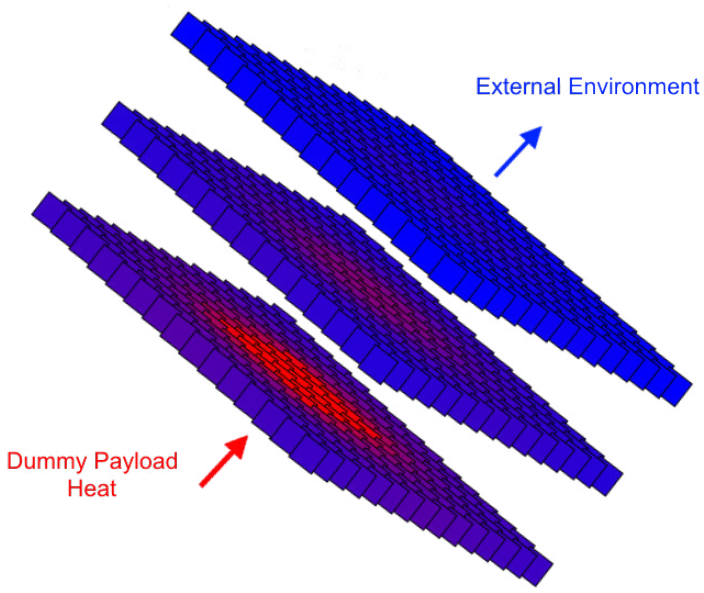

Figure 3.37: Representation of the POLARIS radiator with divided differences method

3.4 Software Design

The experiment software design involves two segments: the flight segment, operating on the on-board *PCM*-3343 SBC, and the ground segment, running on two PCs and connected to the flight segment through the provided *E-Link* system. The Esrange Airborne Data Link (*E-Link*) is a telemetry system that offers a simplified interface for the BEXUS experiments with a standard Ethernet protocol.

The flight segment software autonomously manages the experiment operations and handles the data provided by sensors, storing them into an on-board solid-state memory and sending them to the ground segment through the *E-Link* connection. Moreover, it is possible to override the automatic behaviour of the software by means of a manual control from the ground station. The flight segment autonomously performs the opening and closure of the radiator plates during the flight. Managing the heating subsystem, it also keeps the experiment internal temperature within the desired range, which is pre-configured but can be modified from ground during flight to guarantee more flexibility to the experiment.*Debian* has been chosen as the operating system running on the on-board computer as it is compatible with the *PCM*-3343 platform. The software is developed in *ANSI C* using the *GCC* compiler. *QNX* was the initial choice as the experiment on-board computer operative system, but the lack of real time timing requirements and support for the *PCM*-3343 platform lead the team to switch to *Debian*. The board manufacturer, *Advantech*, also provided hardware libraries for *Linux*.

The ground segment allows a manual control on experiment operations and permits a real time monitoring of data gathered by on-board sensors. Manual control automatically switches off after a chosen time delay unless commands are submitted again as a precaution measure in case of *E-Link* connection malfunctioning. It also stores a backup copy of received data locally for later review. While the on-board software is written in *ANSI C*, the ground segment application and the graphical interface are instead written in *Python*.

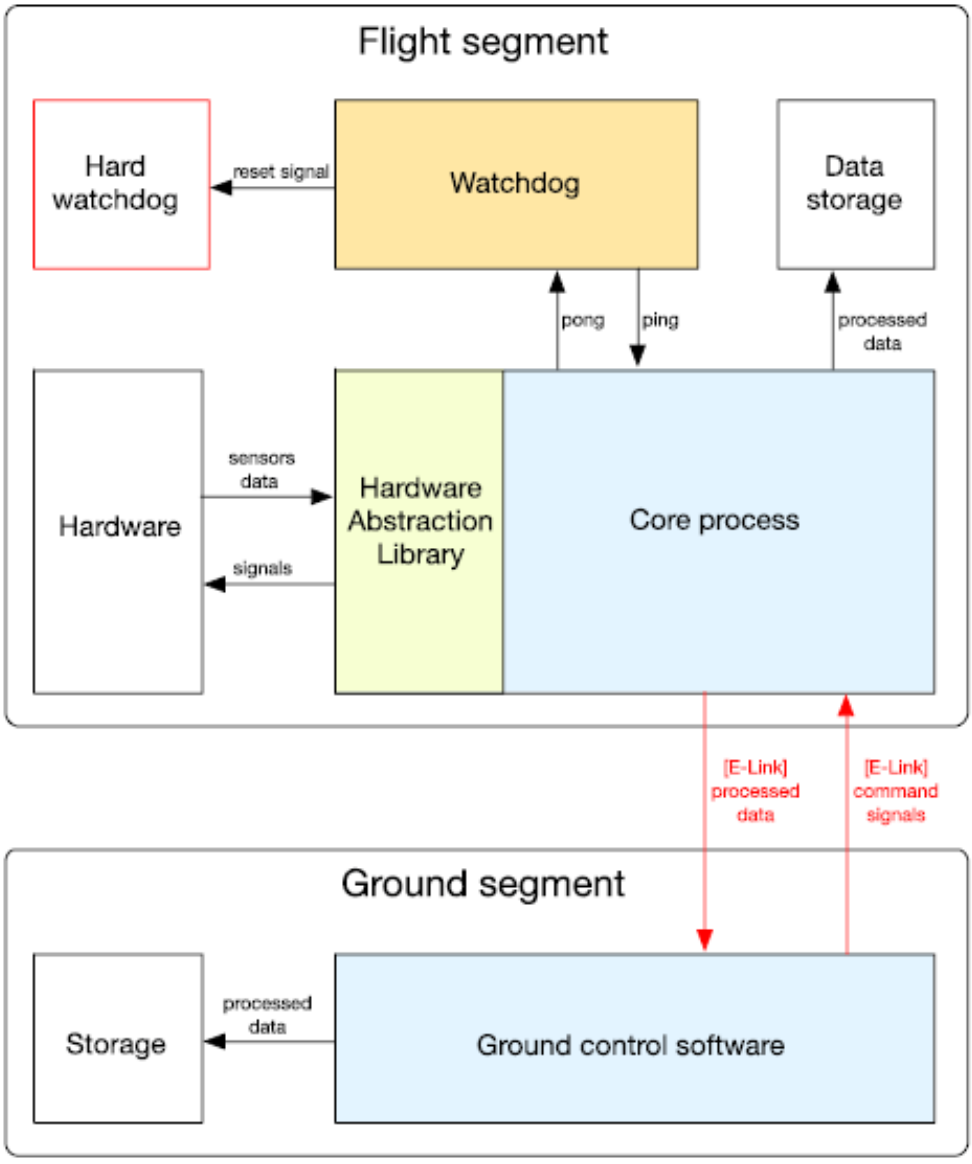

Figure 3.38: Software design concept

3.4.1 Flying Segment

POALRIS Core is the core process of the flying segment and manages the communication both with on-board hardware and the ground segment. POLARIS Core holds records of the system state and is itself a simple finite state machine switching between operational modes, Automatic and Manual, and between different phases of the experiment. The Core process is designed to operate autonomously, but it can also receive manual override commands from ground segment. The Core process employs the *Advantech SUSI* library for *PCM*-3343 board IO functions and the *Sensoray* API for sensors reading. These two library sets are provided by the constructors of the on-board computer and of the data acquisition boards. Sensors data are collected, processed and finally saved locally in the on-board flash memory as well as sent to the ground segment through the *E-Link*. POLARIS CORE also handles UDP and TCP socket communication from and to the ground segment. Through UDP multicast connection, the flight segment is able to stream sensor data to the ground segment while it can receive commands from the ground through TCP connection.

To increase software reliability, watchdogs have been implemented both at software and hardware level. The *PCM*-3343 already has an implemented hardware watchdog that can be easily controlled with the provided libraries. The software watchdog is written in *ANSI C* and is responsible for maintaining and verifying the responsiveness of the core process and, in general, of the whole system. Specifically, POLARIS Watchdog is able to test the responsiveness of the Core process running on-board through a simple TCP socket request. If the process does not respond, it kills and restarts it again. POLARIS Watchdog is launched on system boot as it spawns the POLARIS Core process itself. POLARIS Watchdog also manages the hardware watchdog running on the *PCM*-3343. Thus if POLARIS Watchdog becomes itself unresponsive the whole system is rebooted. After a system reboot, POLARIS Core is able to recover its previous running state from a log file stored on the on-board solid-state memory. Each time the system switches a parameter of its running state, a new version of the log file is updated on the solid-state memory. POLARIS Core is able to choose the most recent version of the log file on system reboot.

POLARIS Core logic is presented in detail in the following process flow charts. Note that for software implementation simplicity, the experiment phases will be divided in 0a, 0b, 1a, 1b, 2a, 2b, 3 where:[1]

- Phases $0a$ and $0b$ represent the initial state of the experiment respectively while the experiment is on the launch pad and in the ascending phase of the flight. The switch from phase $0a$ to $0b$ triggers the counting of the elapsed time of the experiment. When the external pressure drops below a chosen threshold the experiment switches to phase $1a$ (a redundant timed switch has been added in case of pressure sensors malfunctioning). During these phases automatic actuations cannot occur; manual actuations can be performed for testing purposes.

- Phases $1a$ and $1b$ are related to the so called Time Control Loop phase of the experiment (TiCL). During this phase the radiator is tested with timed openings and closures of the plates. During phase $1a$ the plates will be moved between closed and partially separated configurations while during phase $1b$ the plates will be moved between closed and totally separated configurations. A timer switches the system from phase $1a$ to $1b$ and then to phase $2a$

- Phases $2a$ and $2b$ implement the Temperature Control Loop phase of the experiment (TeCL). During this phase, payload temperature readings are used to trigger plates openings and closures. When the temperature exceeds a given range, the SBC triggers an actuation for the radiator. During phase $2a$ the plates move between closed and partially separated configurations while during phase $2b$ the plates move between closed and totally separated configurations. A timer switches the system from phase $2a$ to $2b$ and finally to phase 3

- Phase 3 represents the descending phase of the flight. During this phase the plates are forced to remain closed and the HV subsystem is powered off.

[1]Software phases are numbered from 0 to 6 in the coded C program, but the presented numeration is kept for explanation purposes

The ground segment is also able to force the on-board software to switch to any desired phase at any time. Nominally, the switch between phases $0a$ and $0b$ is manually performed after the balloon lift-off.

POLARIS Core is based on a simple multi-threaded design where periodic tasks with different timings and frequencies are handled by different threads. Synchronization and communication between threads uses shared memory variables and mutexes. Specifically, the Core process runs 4 concurrent threads: Main, Actuations, Sensor Reading and Messages.

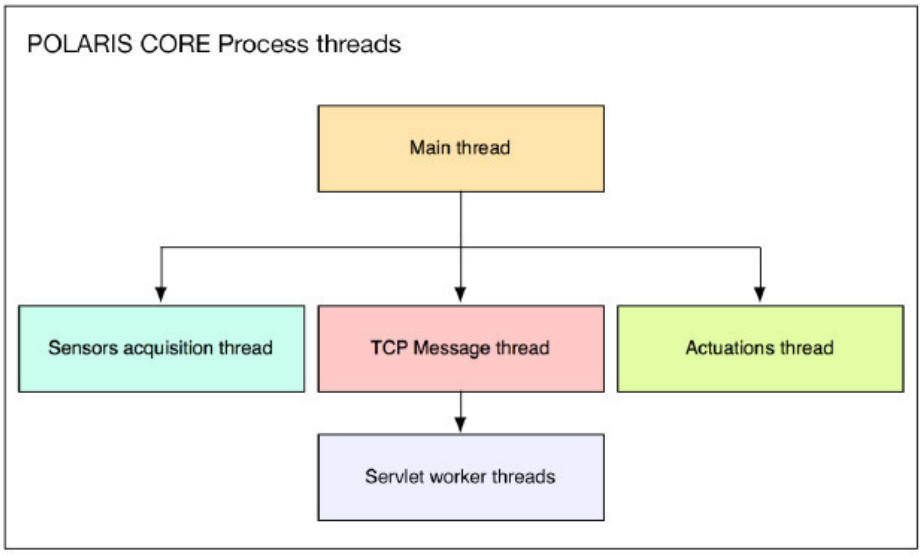

Figure 3.39: Core process threads

3.4.1.1 Main Thread

On start up, the Main Thread initializes the system hardware, reads the initial status file (restore previous system status in case of reboot occurrences), initializes all global variables, sets the *Sensorays* 518 data acquisition boards and spawns all other threads. All memory blocks shared by different threads are allocated and handled by the Main Thread. Every thread shares a mutex with the Main, which locks variables that could be accessed at the same time by both the Main and the thread itself, in order to avoid conflicts due to concurrent data writings.

Afterwards the Main Thread enter in a loop where it checks if any manual command has been received from the ground segment, it handles the system status and, if necessary, updates the log file, it controls experiment phases and finally stores the acquired data and sends them to the ground through the UDP connection. The elapsed time of the experiment is also specified in the UDP message as well as other state variables which allow the ground segment to verify the system status.

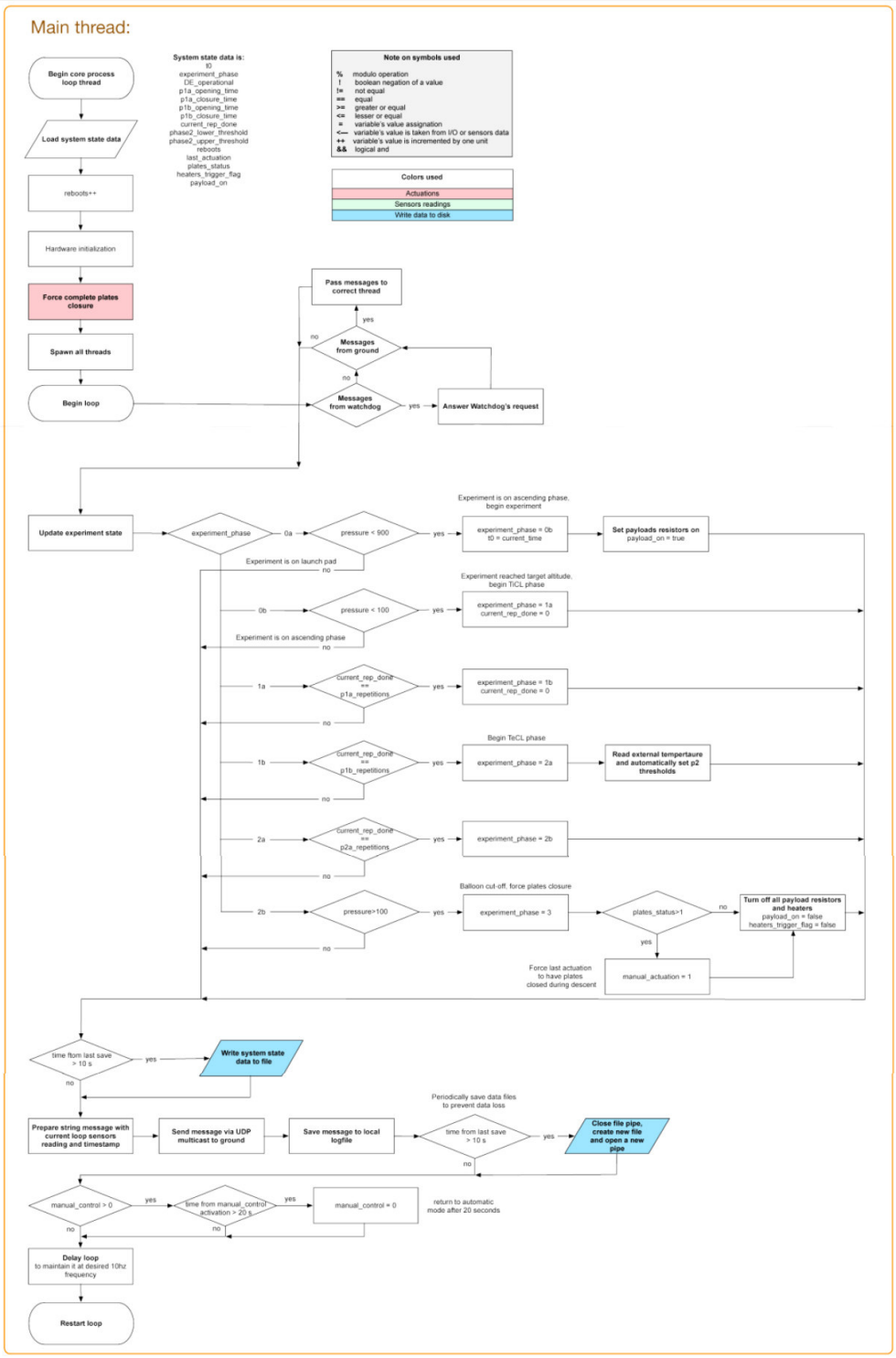

Figure 3.40: Logic scheme of the Main Thread of the on-board software

3.4.1.2 Actuations Thread

Actuations thread handles all the automatic software decisions regarding radiator actuations, experiment heaters activation for internal temperature control and payload heater monitoring and activation. Radiator actuations are performed both by the DE Actuators and the LEM systems. Both actuation systems are controlled by the I^2C port of the on-board computer. The thread can perform four different types of actuations.

Actuation Type 1
Actuation Type 1 brings the radiator to its closed configuration. The Actuation Thread performs the following procedure:

- Turns off the high voltage subsystem (power off DE actuators), moves LEM to position 1 (closed configuration)
- Waits for 5 seconds, than checks optical interrupters signals to detect plates position
- If detected position is not correct, repeats the initial commands: turns off the high voltage subsystem, moves LEM to position 1
- Waits for 5 seconds, than checks optical interrupters signals to detect plates position
- If position is still incorrect, signals failed actuation

Actuation Type 2
Actuation Type 2 brings the radiator to its partially opened configuration employing the LEM system. The Actuation Thread performs the following procedure:

- Turns off the high voltage subsystem (power off DE actuators), moves LEM to position 2 (partially separated configuration)
- Waits for 5 seconds, than checks optical interrupters signals to detect plates position

- If detected position is not correct, repeats the initial commands: turns off the high voltage subsystem, moves LEM to position 2
- Waits for 5 seconds, than checks optical interrupters signals to detect plates position
- If position is still incorrect, signals failed actuation

Actuation Type 3
Actuation Type 3 brings the radiator to its totally opened configuration employing the LEM system. The Actuation Thread performs the following procedure:

- Turns off the high voltage subsystem (power off DE actuators), moves LEM to position 3 (totally separated configuration)
- Waits for 5 seconds, than checks optical interrupters signals to detect plates position
- If detected position is not correct, repeats the initial commands: turns off the high voltage subsystem, moves LEM to position 3
- Waits for 5 seconds, than checks optical interrupters signals to detect plates position
- If position is still incorrect, signals failed actuation

Actuation Type 4
Actuation Type 4 brings the radiator to its partially opened configuration employing the DE actuators. The Actuation Thread performs the following procedure:

- Turns on the high voltage subsystem (power on DE actuators), moves LEM to position 1 (same as closed configuration)
- Waits for 30 seconds, than checks optical interrupters signals to detect plates position
- If detected position is not correct, repeats the initial commands: turns on the high voltage subsystem, moves LEM to position 1

- Waits for 30 seconds, than checks optical interrupters signals to detect plates position
- If position is still not correct, signals failed actuation and performs an Actuation Type 2 (the linear electric motor is used as a backup solution for the DE actuation system)

The Actuation Thread also manages the heating subsystem of the experiment and the dummy payload of the radiator. To maintain the simplicity of the experiment, the heating subsystem is controlled comparing the measured internal temperature with a set of thresholds. The heaters are incrementally powered on as the internal temperature decreases. Thresholds are chosen so that the heating subsystem can be able to maintain the internal temperature of the experiment within the operative range of all its components. The dummy payload nominally works with only two of its three heaters powered on. The software continuously checks the dissipated power ratio from the dummy payload power monitor. If the power ratio goes below a given threshold, the software interprets it as a signal of a failure of one of the heater resistances. Therefore the Actuation Thread powers on the last heater which acts as a redundant backup solution.

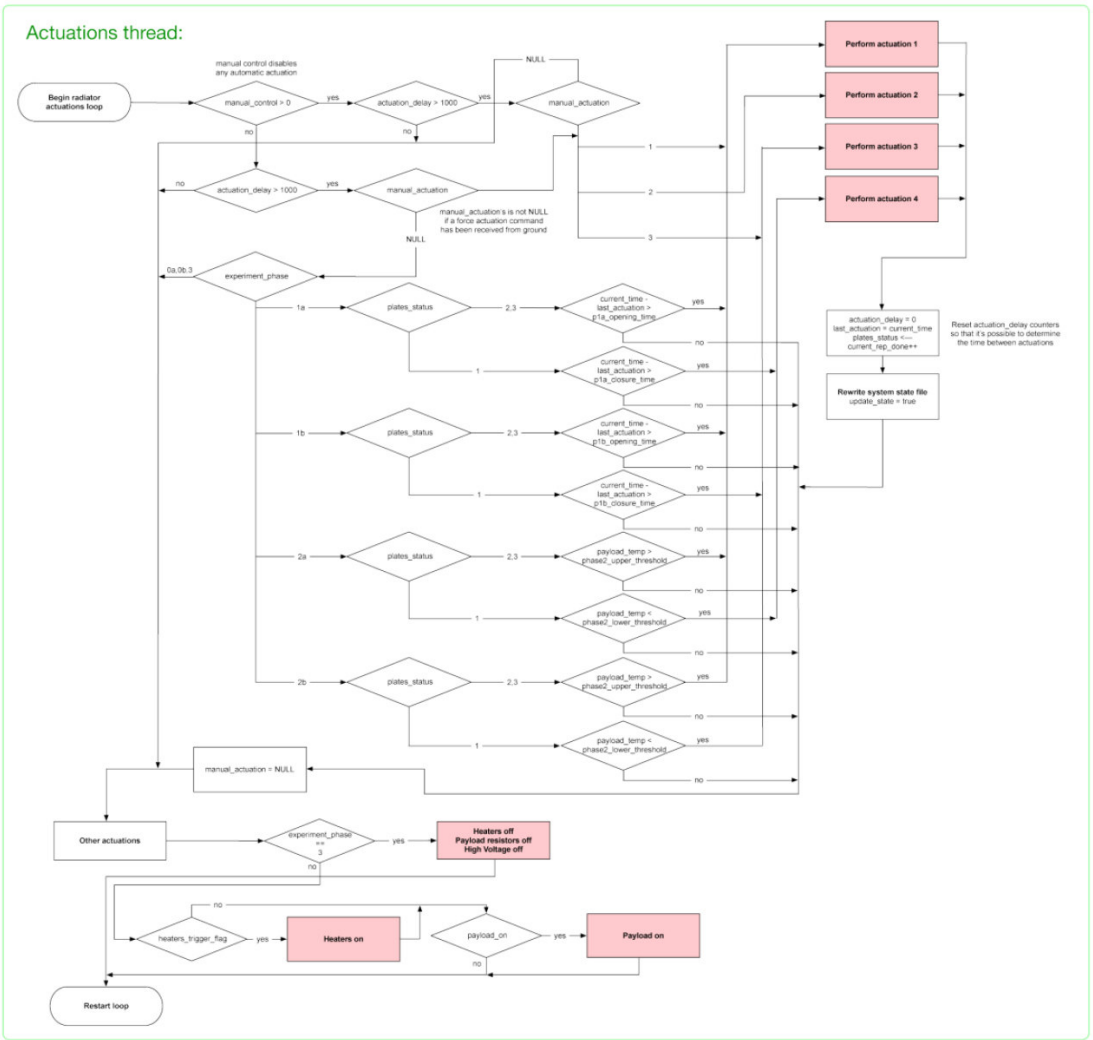

Figure 3.41: Logic scheme of the Actuation Thread of the on-board software

3.4.1.3 Sensor Reading Thread

This thread acquires raw data from experiment sensors and performs conversions and computations to obtain variables values with their proper measure units. Acquired sensors are:

- 8 $PT100$ RTDs placed on the radiator plates
- 2 air pressure sensors
- 2 more $PT100$ temperature sensors (internal and external temperature of the experiment)
- 1 pyranometer (measures incoming radiation in visible wavelengths)
- 1 pyrgeometer (measures incoming radiation in infrared wavelengths, requires two dedicated channels of the DAQ)
- 1 dummy payload power monitor (measures dissipated heat ratio)
- 2 optical interrupters (monitor position of the radiator plates)

All sensors are read through the two *Sensorays* 518, except the two optical interrupters which are read through the GPIO ports of the on-board computer directly. Sensors can be enabled or disabled with a ground command. Hence, when there is a redundant sensor, it is possible to prevent a malfunctioning sensor from influencing the automatic behaviour of the experiment.

Raw data are pushed into a circular queue where the last ten readings are kept. Sensor readings are then taken from the queue discarding highest and lowest values and computing the mean value from the remaining in order to reduce high frequency noise and discard occasional misreadings. Acquired values are then used to compute fundamental values for the automatic control of the radiator and to compute the dummy payload temperature, internal plate average temperature, external plate average temperature and atmospheric pressure.

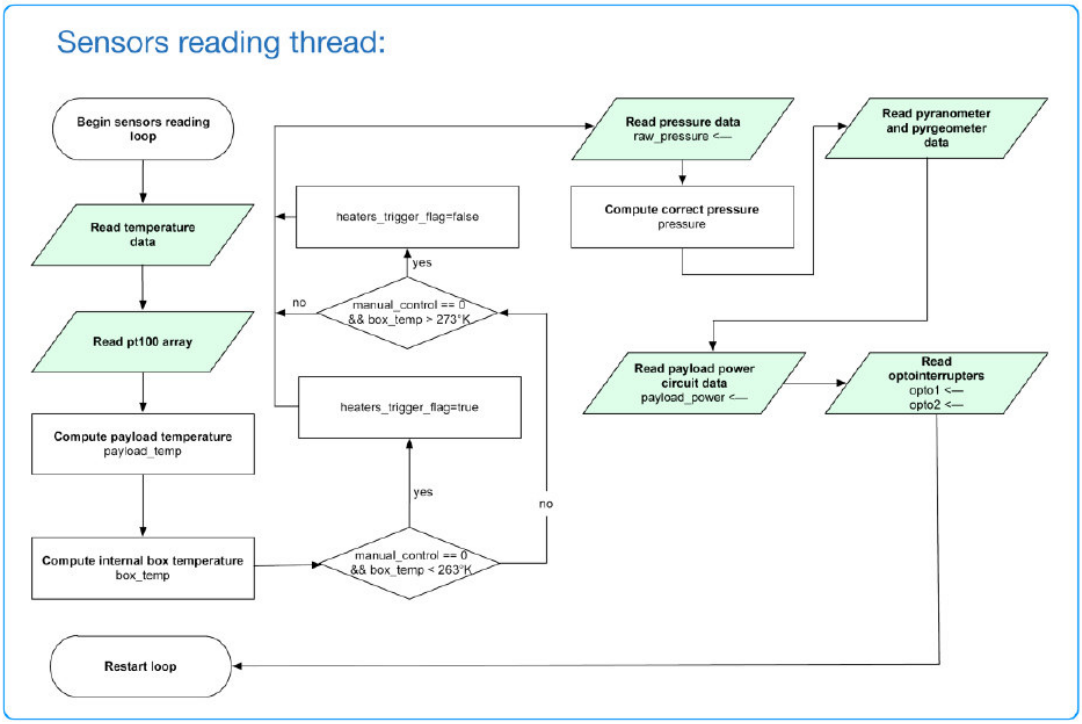

Figure 3.42: Logic scheme of the Sensor Reading Thread of the on-board software

3.4.1.4 Messages Thread

The TCP receiver thread handles the messages sent from the ground segment to the experiment and translates them into commands. Messages are received as integers preceded by an identification code which specifies the purpose of messages (e.g. enabling or disabling a given sensors, switch plates configurations, etc). The Messages Thread then sends received commands to the Main Thread, which forwards them to the appropriate thread.

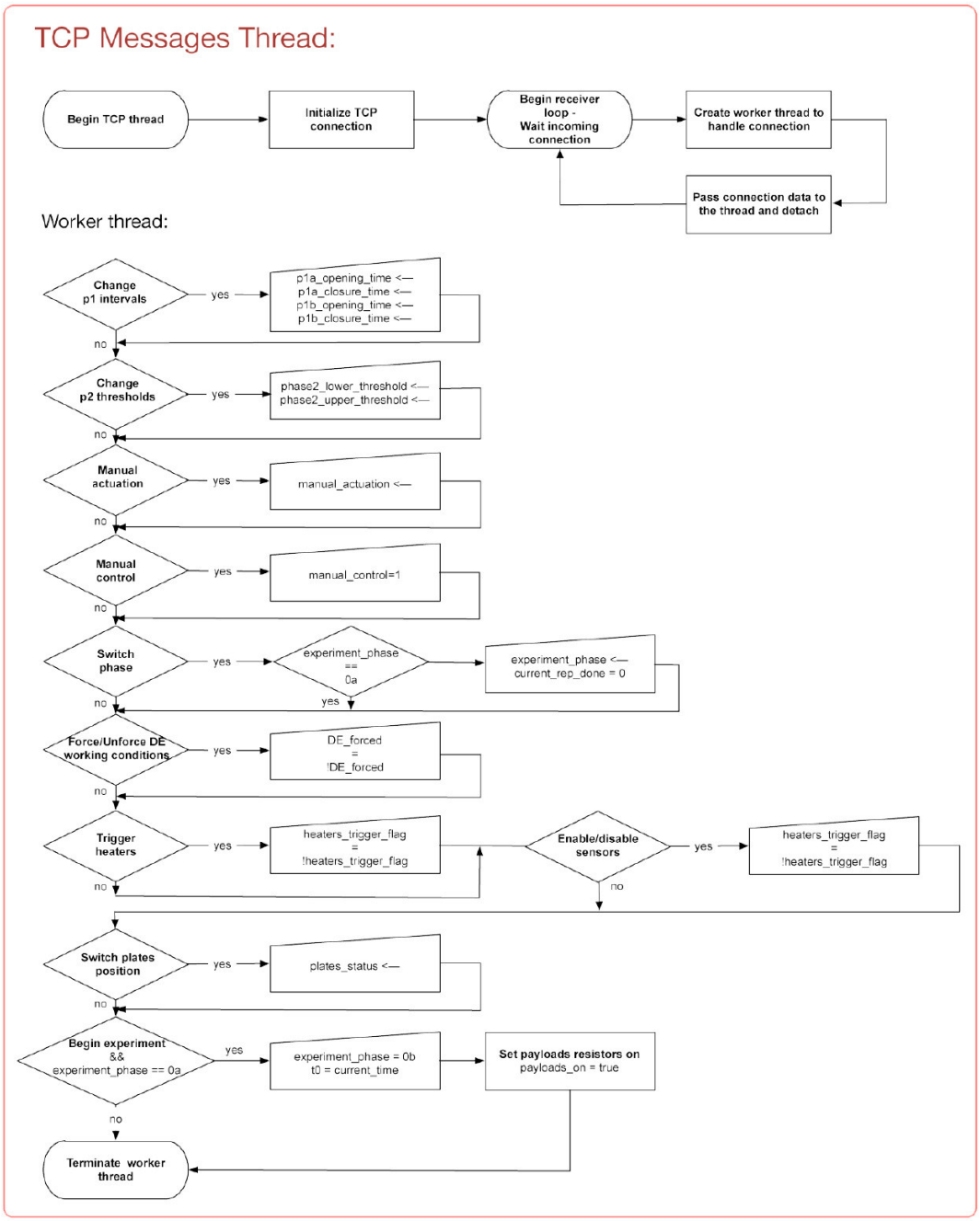

Figure 3.43: Logic scheme of the Messages Thread of the on-board software

3.4.2 Ground Segment

The ground segment software is based on a simple GUI which shows all received data from on-board sensors and all available commands foreseen for manual interaction with the experiment. Ground segment GUI also shows some system status variables such as experiment starting time, elapsed time, experiment phase, etc. Manual operations are implemented to face unpredicted or unexpected experiment behaviour or if any malfunction is detected. Manual controls are provided through simple key buttons on the GUI which can trigger manual mode and perform actuations if needed. Manual commands allow to:

- Begin experiment (switch software phase and set current time as initial experiment time)
- Switch experiment phase (see section 3.4.1 for more details about experiment phases)
- Change timer switch for automatic radiator actuations during phases $1a$ and $1b$ (see section 3.4.1)
- Change temperature thresholds for automatic radiator actuations during phases $2a$ and $2b$ (see section 3.4.1)
- Trigger actuation manual mode, disabling automatic actuations of the radiator
- Force an actuation, the on-board software is forced to perform the required actuation but then it will proceed with its automatic behaviour
- Set DE working conditions, the software does not try to perform DE actuations if DEAs working condition flag is disabled
- Trigger heaters manual mode, disabling the automatic behaviour of the heating subsystem and allowing to switch each single heater on or off manually

- Trigger dummy payload manual mode, disabling the automatic behaviour of the dummy payload and allowing to switch each of its heaters on or off manually

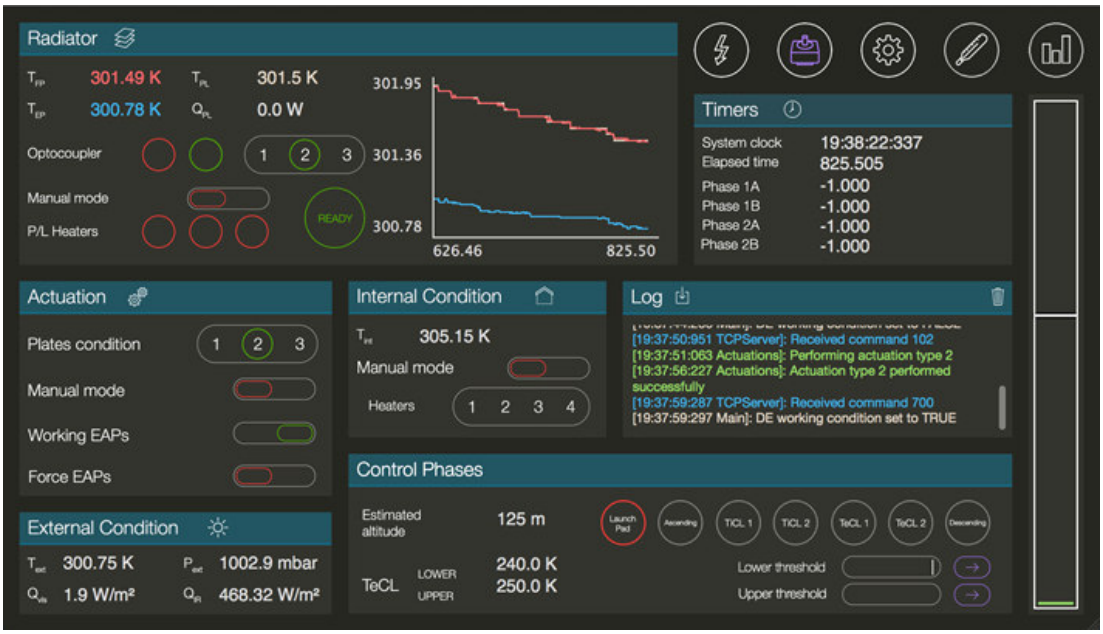

Figure 3.44: POLARIS ground segment GUI

3.5 Experiment Overview

This section summarizes the experiment mass, total dimensions and its electrical interfaces with the BEXUS system.

Table 3.3: Experiment mass and dimensions

Experiment Properties	
Mass [Kg]	16.0
Dimensions [m]	$0.46 \times 0.37 \times 0.36$
Footprint Area [m^2]	0.1702
Volume [m^3]	0.061
Center Of Gravity [m]	$X = 0.226$ $Y = 0.171$ $Z = 0.148$

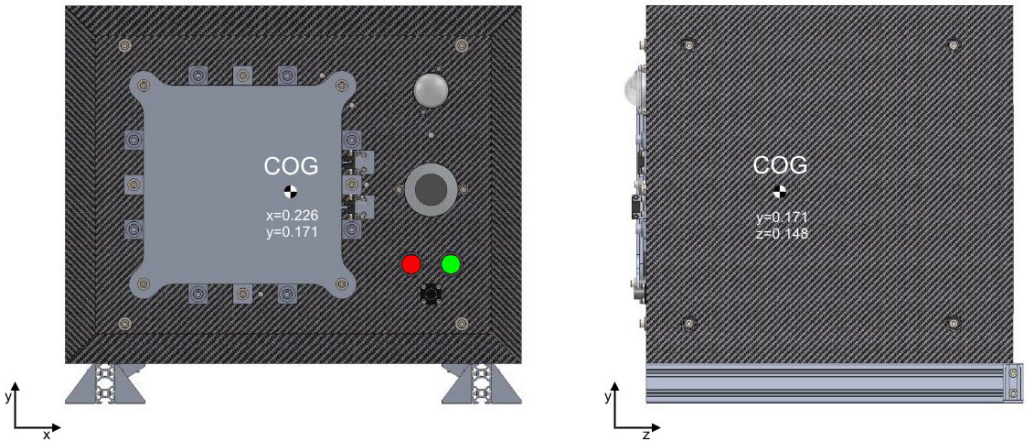

Figure 3.45: Visual representation of the Center Of Gravity of the experiment

Table 3.4: Experiment electrical interfaces

BEXUS Electrical Interfaces	
E-Link Interface: E-Link required	
Number of E-Link Interfaces	1
Data Rate - Downlink	80 $Kbit/s$
Data Rate - Uplink	10 $Kbit/s$
Interface type	RS-232, Ethernet
Power system: Gondola power required, 2 standard battery packs	
Peak power (current) consumption	45 W (1.6 A)
Average power (or current) consumption	32 W (1.2 A)
Power system: Experiment includes batteries	
The SBC features a lithium CR2032 (3 V, 210 mAh) battery for the internal RTC	

Chapter 4

Launch Campaign

From October 3rd to October 13th, the team participated in the experiment launch campaign at Esrange Space Center of the SSC in Kiruna, Sweden. Table 4 outlines the main milestones of the launch campaign. The experiment reached Kiruna disassembled in order to guarantee structure and component integrity during the journey. The first days of the launch campaign were dedicated to assembly and testing of the experiment.

Table 4.1: Launch campaign milestones

Campaign Milestone	**Date**
Earliest Student Arrival	03/10/2014
Begin of Launch Campaign	05/10/2014
Experiment Integration	05-08/10/2014
Earlies Launch Date	08/10/2014
Planned Date of Student Departure	13/10/2014

4.1 Experiment Assembly

On arrival, a work station was assigned to the POLARIS Experiment where the team had the possibility to assemble the experiment and perform some integration tests to verify the experiment compatibility with the BEXUS gondola

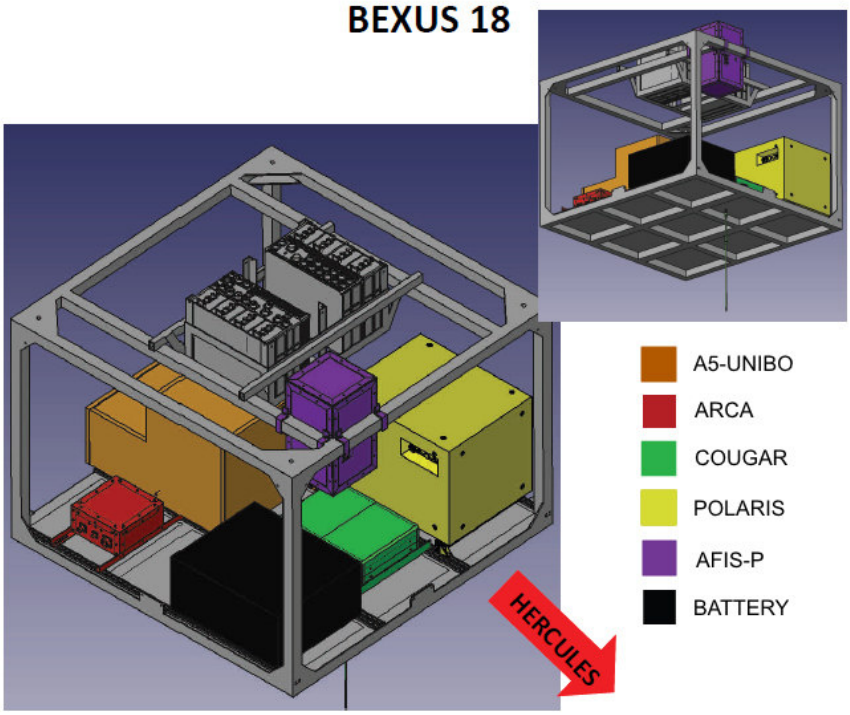

Figure 4.1: Experiments location inside the *BEXUS* 18 gondola. The red arrow indicates the position of the *Hercules* launching vehicle

equipment, in particular with the provided $28\,V$ power supply and the $E-Link$ connection. The team organized the ground segment of the experiment, testing the compatibility with the $E-Link$ connection also with the ground segment of the experiment.

Figure 4.2 summarizes the assembly process of the experiment. First the front face of the experiment was assembled and fixed on the experiment box frame. Then the electronics of the experiment was mounted; the single board computer, the data acquisition boards and the custom PCBs were connected and mounted on the electronics shelf and the latter was fixed to the box frame. After that, the actuation systems were assembled and fixed to the POLARIS Radiator plates. At this point the experiment was powered on and tested through the rear connection panel. Afterwards the thermal insulating walls of the experiment were added to complete the experiment assembly. The effective power consumption and the $E-Link$ connection were verified in collaboration with experts of the REXUS/BEXUS programme and of Esrange Space Center. Finally the experiment was placed and fixed in its position on the $BEXUS$ 18 gondola. Figure 4.1 shows the position of POLARIS Experiment inside the BEXUS 18 gondola among with other students' experiments.

During the assembly and testing of the experiment, the team discovered an issue with the $LEMO$ high voltage connectors which prevent the correct power supply of the DE actuators. Unfortunately these connectors had been delivered only a few days before the launch campaign and they could not be tested properly. For this reason the team decided to connect the DE actuators directly to the high voltage PCB. The only consequence of this issue is a slightly increased complexity in experiment maintenance since the DE actuators can no longer be removed without unsoldering their cables from the high voltage PCB.

The evening before the flight the team was informed that the foreseen flight duration would have been much shorter than the one requested for the experiment due to adverse weather conditions. In particular it was predicted that the wind would soon have driven the balloon towards the Russian border, forcing the premature cut-off of the BEXUS 18 gondola. Hence, the team was forced to rewrite part of the on-board software in order to adapt the experiment behaviour to the shorter mission duration. With reference to section 3.4.1 phases

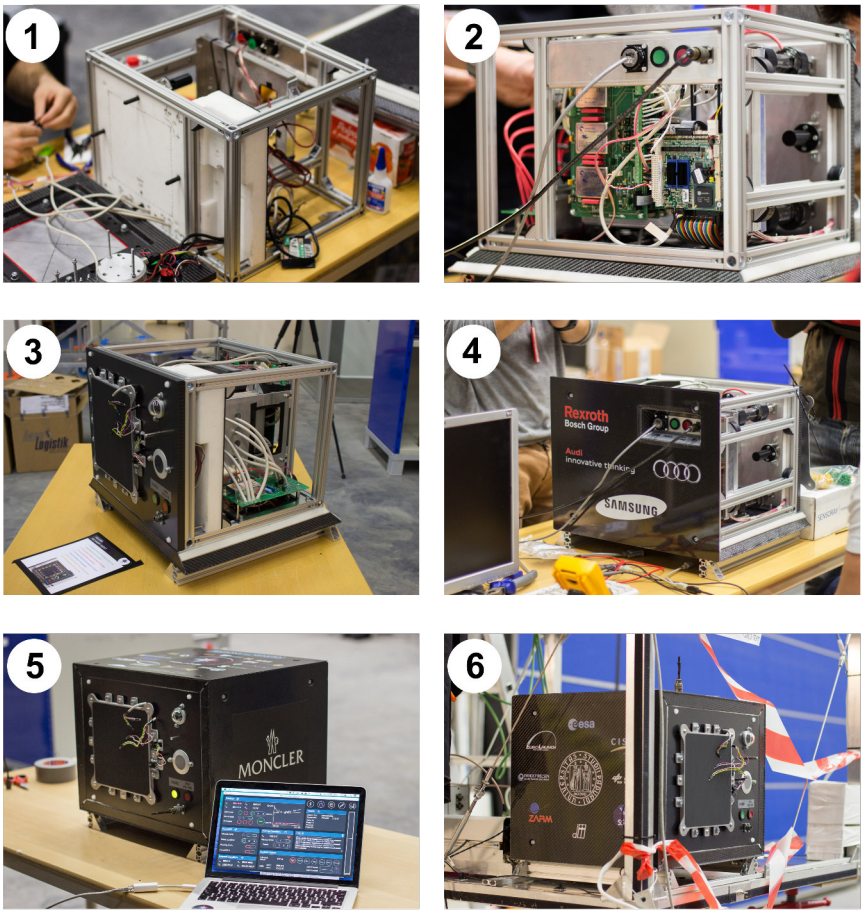

Figure 4.2: Experiments assembly. Mounting of the front face panel [1], mounting of the electronics shelf, of the PCBs and of the SBC and data acquisition boards [2], mounting of the high voltage PCB and of the actuation system [3], testing of the experiment through the rear connection panel [4], POLARIS experiment assembled [5], POLARIS experiment mounted on the $BEXUS18$ gondola [6].

1a and 2a were removed and the experiment was to perform all the actuations with the LEM actuation system only. An additional phase, 2.5, was scheduled to be manually activated 15 minutes before the cut-off of the balloon where the experiment could test the DEAS. It was decided to test the radiator behaviour first and the DE actuators separately. This decision was preferred because of the issues with the of the DE actuators observed in the tests performed during the launch campaign (see section 4.1 for more details). Table 4.2 shows the timeline of the POLARIS experiment from the beginning of the countdown to the end of the flight and highlights the changes previously described. The new software was updated in the flying model and tested during the night before the flight on the spare component of the experiment SBC. The test worked as expected for the whole night, confirming software reliability after the update.

4.2 Experiment flight

Due to problems that occurred during the assembly and the integration process of two experiments that were to share the same gondola as the POLARIS Experiment, the launch was delayed from the earlier launch date (October 8^{th}) to Friday 10^{th} October. The launch countdown began at $06:00am\ GMT+1$. Figure 4.3 shows some of the pre-launch activities performed by the Esrange Space Center personnel: first the gondola pick up and its transportation to the launch pad (1), then the balloon unfolding and inflating (2-3) and finally the balloon ready for lift off on the launch pad.

Figure 4.3: Pre-launch operations. Gondola pick-up [1], balloon unfolding [2], balloon inflating [3], balloon ready for lift off [4].

The release of the balloon (see figure 4.4) happened at $08:48am\ GMT+1$, without any issue. The balloon ascended for two hours until it reached an altitude

of approximately 27200 m above sea level and the floating phase of the flight began. The floating phase lasted one hour and eight minutes until the cut-down of the balloon at $12:00\ GMT+1$. The gondola and all the experiments were retrieved and brought back to Esrange Space Center the day after.

Figure 4.4: Balloon lift off

Table 4.2: Launch Timeline

Time (hh:mm)	**Estimated Height (km)**	**Foreseen Action**
T-05 : 00	0	Last check of the experiment subsystems
T-04 : 00	0	Experiment power on Ground segment and E-link connection test Software phase 0*a* - Start data recording
T-03 : 00	0	Visual check of the LED indicators Team confirms for pick up
T-02 : 30	0	Powering on pre heating circuit
T-01 : 30	0	Team confirms go for balloon unfold
T-01 : 00	0	Turning off pre heating circuit Team confirms go for inflation.
T-00 : 40	0	Team confirms go for launch
T-00 : 20	0	Late access to experiments
T=00 : 00	0	Lift off Software switches to phase 0*b*
T+00 : 20	5	Ascending phase Turn on Dummy payload
T+01 : 30	25-30	Floating phase Start TiCL phase Software switches to phases 1a and 1b
T+03 : 00	25-30	Floating phase Start TeCL phase Software switches to phases 2*a* and 2*b*
T+04 : 30	25-30	Starting pre cut-off procedure Team confirms go for flight termination
T+05 : 00	25-30	Balloon cut-off Software switches to phase 3
T+05 : 20	0	Landing and recovery Experiment physically turned off by recovery crew
T+01 : 30	25-30	Floating phase Start TiCL phase - Software switches to phase 1*b*
T+02 : 15	25-30	Floating phase Start TeCL phase - Software switches to phase 2*b*
T+02 : 45	25-30	Manual switch to software phase 2.5 Team confirms go for flight termination
T+03 : 00	25-30	Balloon cut-off Software switches to phase 3
T+03 : 20	0	Landing and recovery Experiment physically turned off by recovery crew

4.2.1 Failures

Two minor failures occurred during the flight. The first happened 34 minutes after takeoff. The dummy payload power monitor detected the failure of one of its three resistors. This component failure did not limit the experiment performance since the third resistor works as a redundant backup solution and it had been added as a precaution to avoid this kind of problem. The software autonomously recognized the issue and turned on the redundant resistor. After the flight, the failure was attributed to the glue used to fix the dummy payload to the internal side of the first plate which melted during the flight due to high temperature. When the resistor was no longer in contact with the first plate, it overheated until failure. Unfortunately, it was not possible to use a safer fastening method for these components in order to guarantee the flatness of the radiator plates.

The second failure occurred 86 minutes after takeoff. From that moment, the experiment ceased to communicate with the ground segment. After one minute the connection returned and the flying segment indicated that a reboot had occurred. It was not possible to determine a definite cause for this reboot. Most likely the experiment SBC rebooted after a voltage drop from the battery power supply. A software failure or overheating of the SBC processing unit could also have been possible causes but these have been discarded since it was the only reboot during the whole flight and the team never experienced this kind of issue during ground testing (not even in the vacuum chamber).

In both cases, these failures did not limit the experiment performance since a proper solution had been foreseen and implemented and the experiment was able to perform all the required tasks during the whole flight.

4.3 Experiment Recovery

The recovery crew reported that the gondola fell with POLARIS face towards the ground. Figure 4.5 shows the experiment after the recovery of BEXUS 18 gondola and highlights the only visible damage which are some light scratches on the coating of the external plate of the radiator. After recovery, the experiment was disassembled and the compact flash card containing data was removed. Raw

data was then converted into readable form by a script and than used for an initial estimation of the experiment performance. Data immediately showed encouraging results since heat exchange through the radiator changed substantially between different radiator configurations. The experiment was packed fully assembled, except for the compact flash memory card that was previously extracted and prepared for the return shipping. The team made the first raw data evaluation for the post flight meeting presentation.

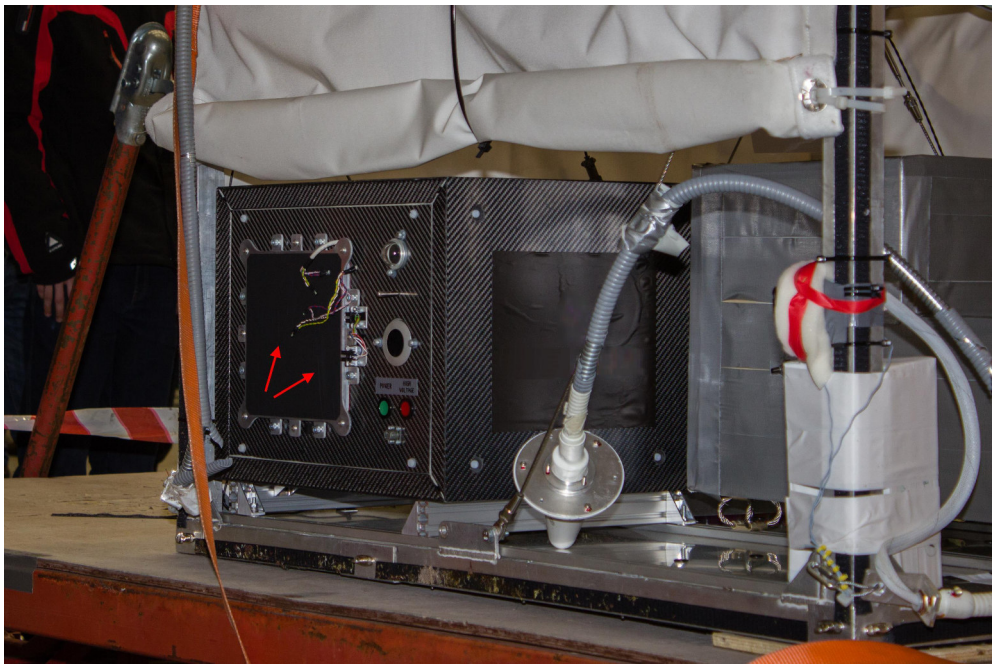

Figure 4.5: POLARIS on the BEXUS 18 gondola after recovery. The two red arrows highlight the only visible damage which are some light scratches on the coating of the external plate

4.4 Flight Results

Due to an incorrect evaluation of air convection coefficient in a low pressure environment made by the team, the experiment faced a much warmer environment during the flight compared to the foreseen one. This forced the team to manually override the automatic behaviour of the experiment for most of the time during the flight. Since the provided $E - Link$ connection with the experiment worked properly during the whole flight, the team was able to control the experiment from the ground segment without any issue and the experiment worked correctly throughout the whole flight.

Gathered data

During the flight, sensors monitored the radiator behaviour in response to environmental conditions and the internal conditions of the POLARIS box. The data acquisition process worked as expected during most of the flight. Only for a brief period at the end of the floating phase of the flight, temperature readings on the external plate of the radiator exceeded the foreseen threshold for that value. The software was designed to discard implausible data and hence those temperature data were lost for a brief period. Anyhow, from the ground segment of the experiment the team was able to change the threshold and hence to restore the data acquisition process correctly. The missing data period is highlighted in figure 4.9. Anyhow, lost data could be easily evaluated with an interpolation of the temperature trend in that period since the missing interval was really short and the temperature was increasing regularly during that period.

The gathered data and results obtained from the stratospheric balloon flight are presented and briefly discussed in the following figures.

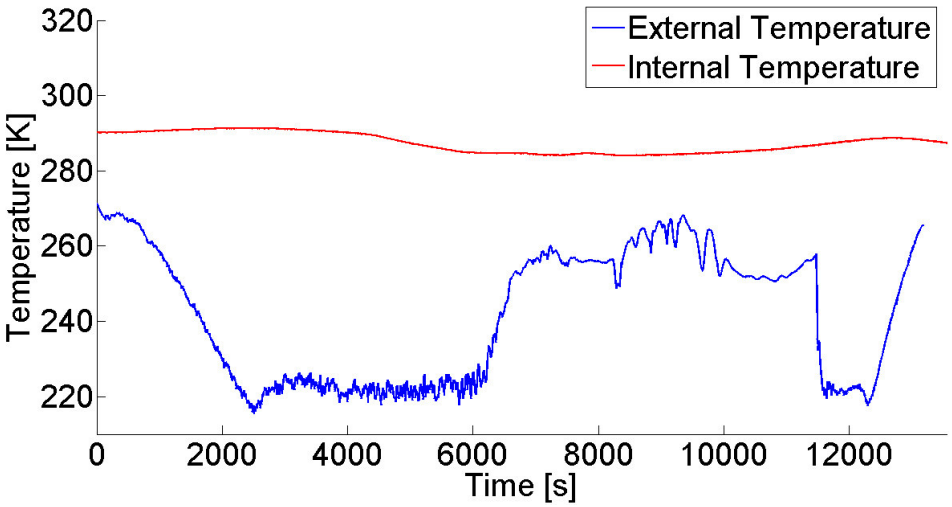

Figure 4.6: Internal and external measured temperature profiles during the flight. The internal value refers to the temperature inside the POLARIS box while the external value refers to the air temperature outside the experiment. It is possible to notice that the thermal insulation and the heating subsystem of the experiment were able to maintain the internal temperature of the experiment within the operational range of all its components.

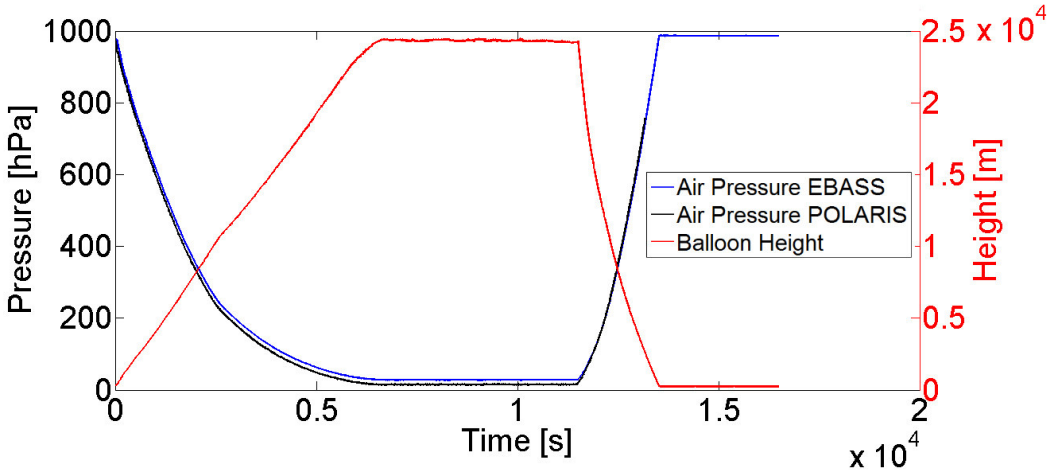

Figure 4.7: Air pressure measured from POLARIS Experiment compared to the value measured from the *EBASS* sensors. Pressure readings were used by the on-board software to obtain a rough evaluation of the balloon height and hence to autonomously determine the starting of the floating phase of the flight.

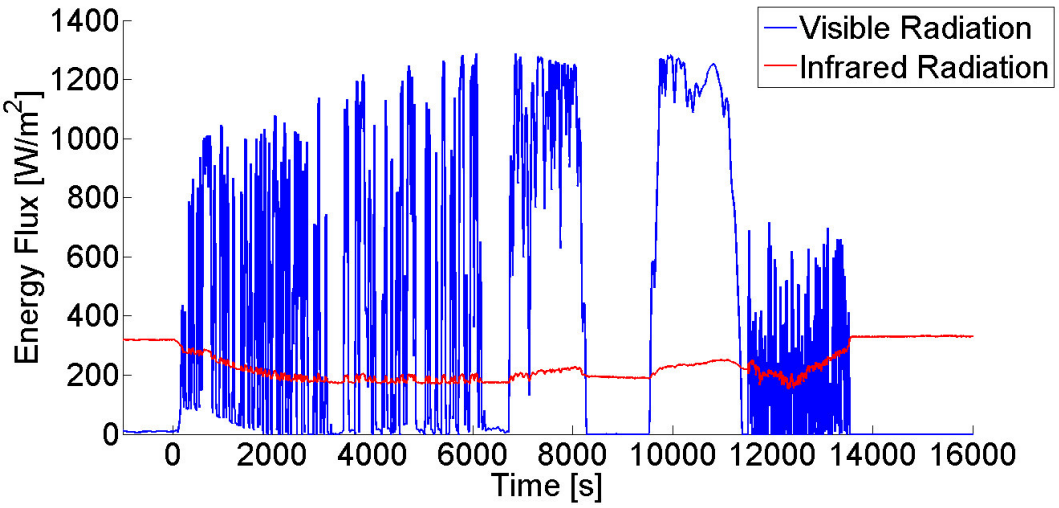

Figure 4.8: Incoming visible and infrared radiation during the flight. The red profile represents the IR radiation. The IR radiation decreased during the ascending phase and stabilized itself during the floating phase. This can be explained with the decreasing view factor of the Earth surface from the ascending experiment. The blue profile represents the incoming visible radiation. Most of this radiation came directly from the Sun while a small amount was reflected toward the experiment by Earth albedo. During the floating phase of the experiment (from 6500 Ms to 11500 s), it is possible to notice the revolution period of the $BEXUS$ 16 balloon. The revolution periodically exposed the experiment to the Sun and in the opposite direction. As a result, the pyranometer measured alternating periods of high light exposure and darkness.

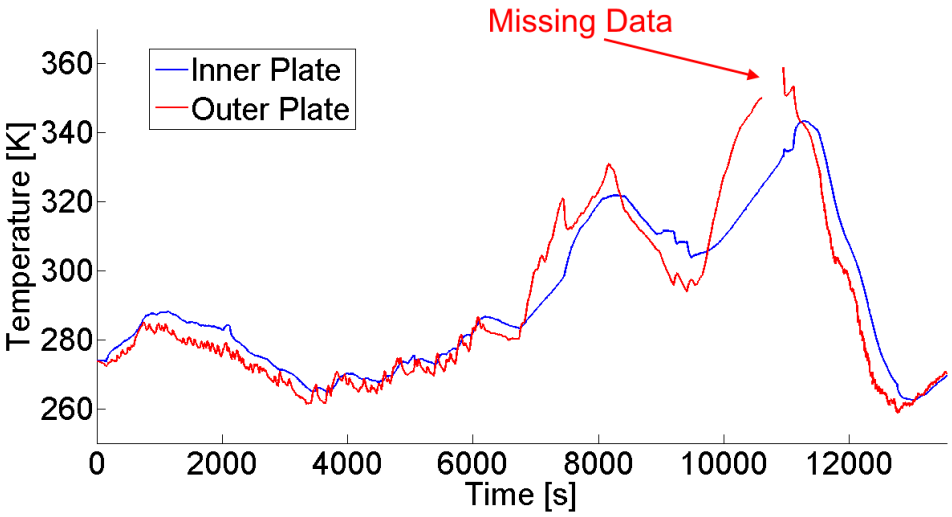

Figure 4.9: Temperature profiles on the internal and external plates of the radiator during the floating phase of the flight. The missing data period is highlighted. Data loss was due to the warmer external conditions faced by the experiment with respect to the team forecast and due to an upper threshold for plausible data in the software. Software was modified during the flight from the ground segment and the team was able to raise the threshold.

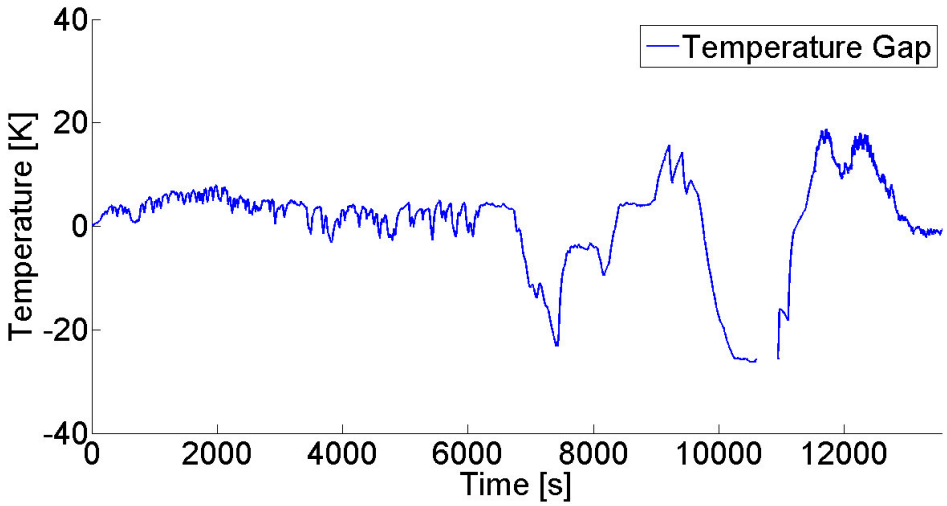

Figure 4.10: Temperature gap between the internal and external plates of the radiator during the whole flight. It is possible to notice the difference between the ascending phase of the flight on the left and the floating phase on the right. The temperature gap in the ascending phase remains close to zero since the radiator was closed during the ascent. The radiator started its actuations with the beginning of the floating phase, resulting in a greater amplitude in the temperature gap between the plates while they were separated from each other.

Updated numerical model

The thermal simulations carried out during the experiment preparation in order to foreseen the POLARIS radiator behaviour were severally affected by the bad estimation of the air convective heat transfer coefficient. A new estimation of this coefficient has allowed to achieve a far more precise estimation of the radiator behaviour. Moreover the simulations have been updated replacing the estimated environmental condition and the incoming thermal loads with values measured during the flight. Figure 4.11 shows a comparison between the results obtained with the new numerical simulations and the data gathered during the flight. More developments on the numerical model are currently under studies to further increase its reliability.

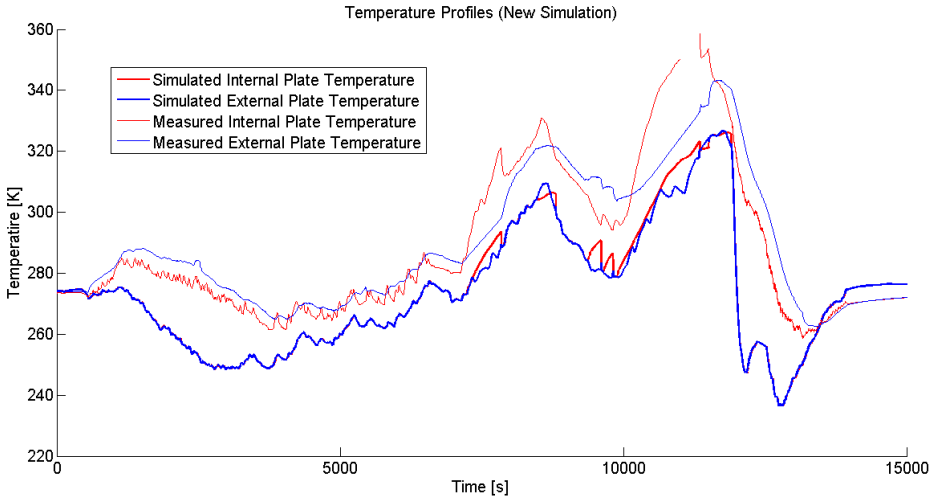

Figure 4.11: Comparison between measured temperatures on the radiator plates and the new numerical model

Chapter 5

Conclusions

POLARIS radiator was tested under an extremely variable environment and its configuration influenced the thermal resistance between the dummy payload and the external environment as expected. The dielectric elastomer actuation system did not develop enough force to perform an actuation for the radiator plates. The cause was probably an high friction coefficient between the ball bushings and the plates rods due to inevitable temperature gradients and differential temperature dilatations of these components during the flight. The stronger linear electric motor was able to perform all the actuations needed during the flight without any additional issue.

POLARIS software was not developed for the warmer environmental conditions that the experiment faced. For this reason the team decided to manually achieve the second objective of the experiment which aims to maintain the dummy payload temperature within a desired range of temperatures, deactivating the automatic behaviour of the experiment during part of the flight. The team was able to maintain the dummy payload temperature within a gap of 6 K for several minutes before the gondola cut off.

From an operative point of view, the experiment survived the stratospheric flight and was able to perform all planned tasks correctly. Two minor failures occurred during the flight but the experiment design was tolerant to these failure and hence the experiment performance were not reduced.

In conclusion, the flight conditions were not the best to perform a quantitative test on the radiator performance, but the flight was a great test bench for the

whole system because of the extreme different conditions faced by the experiment. This encouraging results confirm that the radiator has the capability to fulfill its duty and has the potentialities to be used for an active thermal control device for space or planetary probes. Moreover this flight proved that the experiment was correctly designed to operate in a stratospheric environment and it was able to avoid single points of failure without reducing the experiment performance.

Nomenclature

Acronyms

API Application Programming Interface

ASA Autonomous Spring Actuation

ATC Air Traffic Control

BEXUS Balloon EXperiment for University Students

COG Center Of Gravity

COTS Commercial Off-The-Shelf

DAC Digital to Analog Converter

DC Direct Current

DE Dielectric Elastomer

DEAS Dielectric Elastomers Actuation System

EAP ElectroActive Polymer

EBASS Esrange BAlloon Service System

EMI ElectroMagnetic Interference

GPIO General Purpose Input Output

GPS Global Position System

GUI Graphical User Interface

HV High Voltage

I^2C Inter-Integrated Circuit

IC Integrated Circuit

IO Input-Output

LEM Linear Electric Motor

MLI Multi-Layer Insulation

NTC Negative Temperature Coefficient

PCB Printed Circuit Board

$POLARIS$ POLymer-Actuated Radiator with Independent Surfaces

$REXUS$ Rocket EXperiment for University Students

RTC Real-Time Clock

RTD Resistance Temperature Detector

SBC Single Board Computer

TCP Transmission Control Protocol

$TeCL$ Temperature Control Loop

$TiCL$ Time Control Loop

UDP User Datagram Protocol

WCC Worst Cold Case

WHC Worst Hot Case

Organisations

DLR Deutsches zentrum für Luft und Raumfahrt (German Aerospace Center)

ESA European Space Agency

MORABA MObile ROcket BAse

SNSB Swedish National Space Board

SSC Sweden Space Corporation

ZARM Zentrum für Angewandte Raumfahrttechnologie und Mikrogravitation (Center of Applied Space Technology and Microgravity)

Bibliography

BEXUS User Manual. EuroLaunch, 2014. 9, 12

REXUS/BEXUS website: www.rexusbexus.net 5, 9

D. G. Gilmore, *Spacecraft Thermal Control Handbook*. American Institute of Aeronautics and Astronautics, 1994. 49

R. Zang. *Development of Dielectric Elastomer Actuators and their Implementation in a Novel Force Feedback Interface*. PhD thesis, Swiss Federal Institute of Technology, 2007. 4

D. Paganini et al., *A New Concept of Variable Resistance Radiator*. IAC-14-C2.P.28, 65th International Aeronautical Congress, Toronto. 2014.

D. Paganini et al., *POLARIS Experiment: data collected during the stratospheric flight on the balloon BEXUS 18*. 22nd ESA PAC Symposium on European Rocket and Balloon Programmes and Related Researches, Toronto. 2014.